LONG-RANGE HIGH-THROUGHPUT WIRELESS COMMUNICATION USING MICROWAVE RADIATION ACROSS AGRICULTURAL FIELDS
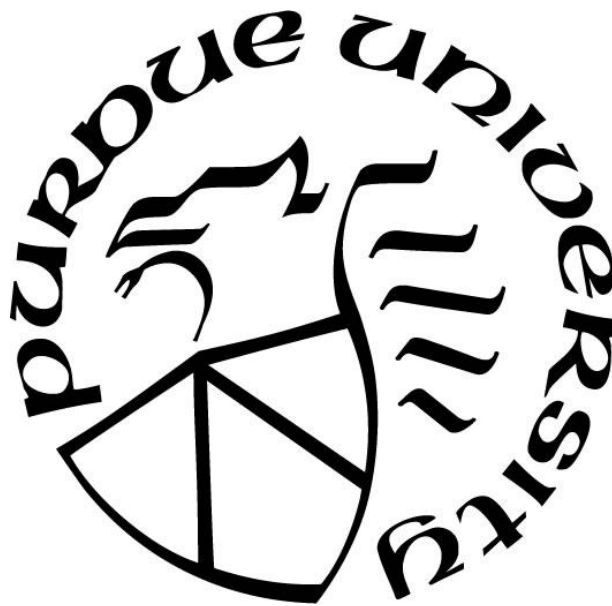
by

Paul Christian Thieme

A Thesis

Submitted to the Faculty of Purdue University

in Partial Fulfillment of the Requirements for the degree of

Master of Science in Agricultural and Biological Engineering

School of Agricultural and Biological Engineering

West Lafayette, Indiana

December 2019

THE PURDUE UNIVERSITY GRADUATE SCHOOL
STATEMENT OF COMMITTEE APPROVAL

Dr. Dennis Buckmaster, Chair

School of Agricultural and Biological Engineering

Dr. Robert M. Stwalley, III

School of Agricultural and Biological Engineering

Dr. James V. Krogmeier

School of Electrical and Computer Engineering

Approved by:

Dr. Nathan S. Mosier

Dedicated to My Family

ACKNOWLEDGEMENTS

From its conception, this research project was aided by innumerable people at each step in the research process. It is not possible to mention each party that helped along the way, and so I would like to give a general acknowledgement to all of those who aided in the execution of this project. However, I would like to mention those with outstanding contributions that were critical to the success of the project here.

First and foremost, to my Lord and Savior Jesus Christ, His Father, and the Holy Spirit for guiding me in my pursuits to this point. He has given me the perseverance, wisdom, and skills needed to complete both this task and those needed to obtain this degree.

To my family and friends for supporting me through late nights, busy weekends, daunting tasks, and who occasionally lent a hand when it was needed. In particular I would like to mention my longtime friend Ian Andrew Ahner from the Missouri University of Science and Technology, whose experience in RF circuit design and prototyping was critical in the construction of some of my research systems.

To the members of my committee listed above, whose guidance and input were invaluable when decisions needed to be made considering proper data collection practices, experiment design, paper writing, and other considerations regarding research practices with which I had relatively little experience.

Finally, to various staff and associates of Purdue University - in particular Bob Henning, RF Engineer and transmit site manager for WBAA, who gave me nearly unlimited access to WBAA's broadcast tower on which my research equipment was mounted. I also wish to mention the staff of the Throckmorton Purdue Agricultural Center (TPAC), the research farm on which WBAA's tower is located and where my research was conducted, for allowing me to conduct my research amidst their daily farm operations and for being continuously available whenever I needed help.

TABLE OF CONTENTS

LIST OF TABLES

LIST OF FIGURES

ABSTRACT

Over the past three decades, agricultural machinery has made the transition from purely mechanical systems to hybrid machines, reliant on both mechanical and electronic systems. As this transformation continues, the most modern agricultural machinery uses networked systems that require a network connection to function to their full potential. In rural areas, providing this network connection has proven difficult. Obstacles, distance from access points, and incomplete coverage of cellular connection are all challenges to be overcome.

"Off the shelf" commercial-grade Wi-Fi equipment, including many products from Ubiquiti like the Bullet M2 transceiver and the PowerBeam point-to-point linking system, as well as antennas by Terrawave, Crane, and Hawking, were installed in a purpose-built system which could be implemented on a production farm. This system consisted of a tower-mounted access point which used an antenna with a 65° beamwidth, and the test included distances up to 1150 meters in an agricultural setting with corn and soybeans. Some sensors were stationary and the other platform was a tractor following a path around the farm with both 8dBi and 15dBi gain antennas. Through all tests, throughput never dropped below 5 Mb/s, and the latency of successful connections never exceeded 20ms. Packets were rarely dropped and never accounted for a significant portion of all packet transmission attempts. Environmental effects like immediate precipitation, crop heights, recent rainfall, and ambient temperature had little or no effect on wireless network characteristics. As a result, it was proven that as long as line-of-sight was maintained, reliable wireless connectivity could be achieved despite varying conditions using microwave radiation. Network throughput was marginally affected by the change in free space path loss due to increased distance between the access point and the client, as well as travel by the mobile client outside the beamwidth of the access point.

By enabling this coverage, it is hoped that the implementation of new agricultural technology utilizing a live network connection will progress more rapidly.

1. INTRODUCTION

1.1 Background

The world's population has been increasing at an exponential rate and is expected to reach 10 billion people by 2050 (Jean-Christophe, 2013). At the same time, farmland is being consumed by increased demand for housing, business space, and land requirements for the expansion of urban areas. These, combined with increasing pressure from the public to adopt more sustainable agricultural practices, are putting enormous pressure on the world's agricultural industry. In order to combat these pressures engineers, farmers, and scientists alike have been developing new methods of food production. Examples of these include the adoption of no-till farming, the implementation of diesel exhaust fluid (DEF) to reduce oxides of nitrogen (NOx) emissions from agricultural engines, the adoption of genetically modified organisms (GMOs) to increase specific yield and favorable characteristics like drought resistance and pest resistance, and the development of new machinery in recent years to reduce soil compaction and to increase the soil's longevity as a viable bed for crop growth. These mechanical and chemical innovations have been coupled with the emergence of electronic systems in agriculture as a means of increasing efficiency and capability in the field. Such systems began with the use of primitive computers to control engine operations in the form of engine control units (ECUs) in the 1980s, continued into the use of machine-wide controller area networks (CAN) to enable communication between the tractor and implement in the 1990s, and evolved further into data collection and analysis systems for data on the CAN in the 2000s. Most recently in the 2010s, this data has been moved from the machine to the cloud and has become accessible from remote locations, enabling the mass collection of real-time data to a centralized location for easier storage and analysis, for example John Deere's JDLink™ technology (John Deere and Company, 2018) or the Open Agricultural Technology and Systems (OATS) Center's ISOBlue system (Purdue University Open Agricultural Technology and Systems Center, 2018). This has been accompanied by an explosion of independent sensors for use apart from a vehicle, such as soil moisture sensors, cameras, nutrient sensors, monitors for livestock, and more. This collective group of internet-enabled sensors for data collection has been referred to as the Internet of Things (IoT). The purpose of connecting these systems of data collection to the internet was to

11

centrally aggregate data for ease of analysis and to enable real-time monitoring of machines for diagnostic and error reporting purposes. (Jean-Christophe, 2013) (Zhang, 2015)

The capability to move data in this way is solely dependent on a stable internet or intranet connection. To help fill this need, supporting technologies have been developed like LoRaWAN (LoRa Alliance, 2018), Zigbee (Zigbee Alliance, 2018), SIGFOX (Sigfox, 2018), and RPMA (Ingenu Inc., 2018). Companies like Solinftec (Solinftec, 2018) are designing and deploying wireless networks to rural areas for the purpose of connecting far-off equipment. Satellite connections are being made available in certain instances for limited data transfer, but in a time of such rapid growth, are all needs being met? There has been exponential growth in research for wireless standards pertaining to IoT, like those mentioned above. However these are intended for low data rate systems and small amounts of data transfer per session. Technologies like LoRaWAN were designed for small sensors, and they do not provide enough bandwidth for use on agricultural machines attempting to send CANBUS or other real-time data. Mature technologies that could support this level of data throughput exist in the forms of cellular networks and satellite clusters. Unfortunately, with data-only cellular plans for IoT pricing above $30 per month, both of these options are prohibitively expensive for farmers wishing to operate many machines. Thus, there is a need for a technology that is able to connect to agricultural machinery at long distance, with enough throughput to send data like CANBUS or other diagnostic data, at low cost.

It is common to have wireless internet via Wi-Fi in public places, in places of work, and at home. With the number of places that Wi-Fi can be deployed, a vast and diverse set of equipment has been developed by many companies to make use of the industrial, scientific, and medical (ISM) 2.4Ghz band on which Wi-Fi is based. Because of this, it is now possible to obtain Wi-Fi equipment tailored to the needs of the space, from a living room to a football stadium. Since there is equipment available that was engineered to bring Wi-Fi to large spaces, research should be conducted that assesses its ability to provide a wireless connection in agricultural settings. This research program was designed to remedy this deficiency.

1.2 Objectives

The overarching goal of this project was to determine whether a reliable 2.4Ghz Wi-Fi system could be created from off-the-shelf components that could service an area large enough to contain production crop fields through a growing season. If this goal could be accomplished, it would show that there is a way for farmers to create their own wide-area wireless network without the need for cellular connectivity. Assessing progress toward this this goal required measuring the network properties themselves, which have thresholds of utility. For this work, these conditions were:

1.   maintain 1 Mb/s throughput capability;
2.   present latency to the network of less than 500 milliseconds; and
3.   equipment able to endure prolonged outdoor / agricultural use.

Of these conditions, the first was that the network had to have a throughput capacity of at least 1 megabit (Mb/s). This stipulation was implemented to ensure that any client needing to support a more information-heavy connection, such as remote access by a technician could do so. Additionally, there needed to be less than 500 milliseconds of lag. Remote diagnostics of vehicles exist today, and with remote operation of vehicles projected to come in the near future, it is vital that latency be kept to a minimum for safety. Finally, it was required that these characteristics be sustained throughout the growing season. While capacity and latency were being measured, effects on these properties by the height of crops throughout the growing season and weather were measured. Thus, the objectives of the project were to:

1.   construct and deploy a system capable of meeting the 1Mb/s
       throughput and 500ms latency requirements;
2.   determine the effect of antenna gain on network properties;
3.   determine if weather affected network properties; and
4.   determine if network properties changed over the growing season.

2. LITERATURE REVIEW

While planning the systems and methods used in this work, inspiration often came from existing research done in the area, and from current technologies. By examining the work of others in measuring wireless propagation characteristics and connectivity in agricultural environments, more informed decisions could be made about equipment selection, measurement techniques, and system design. In this chapter many common practices and typical measurements related to connection testing in agricultural settings are discussed, and examples of others who have performed similar research are given.

When speaking of current wireless research in agriculture, it is important to be familiar with some of the current wireless standards in place. The majority of these standards used in agriculture focus on low-power long-range communications, with few having been designed for high-throughput connections. Examples of these low-power long-range communications standards are the LoRa Wide Area Network (LoRa WAN) and the Zigbee protocol. These were designed to operate with battery-powered wireless sensor networks like distributed field sensors. (Antonis Tzounis, 2017) As such, their focus is on energy efficiency, effective data transmission, and range. They utilize a very narrow bandwidth, traditionally in the 900MHz band but also occasionally in the 2.4GHz ISM band and the 400MHz ISM band, and therefore have very poor data throughput ability. Real-Time Kinematic connections (RTK) are also very narrow bandwidth signals, and are used to add accuracy to GPS-enabled devices through the use of a stationary ground-based beacon. These signals are intended to be a reference for navigation however, and are not expected to carry large amounts of data.

Other technologies enable high-throughput technologies that are often used in agriculture. The most prevalent of these is 2.4GHz Wi-Fi, under the 801.11b/g/n standards. This protocol is ubiquitous in laptop, phone, and mobile device communications. It also carries the misconception that it is range limited to several dozen meters, as shown in Table 2 of Tzounis et al. (Antonis Tzounis, 2017), where a maximum range of 100m is specified. In reality, the protocol has much less to do with useful range than the amount of RF power used and the selection of hardware. This is why communications testing is so vital in agricultural use.

2.1 Signal Measurements

For all wireless communication measurements and testing, some sort of signal measurements are taken to determine the strength of the connection. These measurements can take the form of the received signal strength index (RSSI), field strength, or other data-based metrics like throughput. Each measurement provides a different measure of signal usability and as such are used in different ways. For example, the most basic common measure of a signal's strength is its RSSI. Li et al used the RSSI as a measure of signal strength for transmitters below the canopy in a wheat field (Z. Li, 2010). Instead of using commercial 2.4GHz network hardware, custom 2.4GHz transmitters were used to broadcast data packets from omnidirectional antennae. A spectrum analyzer was used to visually display the strength of each transmitter's signal at distances up to 130m. By using this method, loss due to interference could be directly observed by comparing signal strength provided by the spectrum analyzer. This method does not incorporate data encoding, error reporting, or two-way communication between the transmitter and the receiver, and is therefore simply a direct measurement of signal strength.

On top of a carrier signal, data encoding standards could be implemented like is done in Wi-Fi (IEEE 802.11), LoRA, or other communications protocols. Thus, measurements of signal strength could be made after this encoding stage, as was done by Darr et al. (M. J. Darr, 2008) at Iowa State University. In their work, they implemented the Zigbee protocol on a 2.4GHz carrier to transfer data from sensors distributed throughout a concentrated animal feeding operation (CAFO) for poultry. These indoor measurements were made with two commercial Zigbee-enabled sensors, arranged in a point-to-point configuration instead of a simple transmitter-receiver setup as described previously. With the change in configuration came the ability to measure the received signal from each sensor on the opposite sensor, including a measurement of packet loss and data handling capability. Results from this test yielded a measurement more suitable for predicting data handling capacity of a wireless link as opposed to a raw measure of RF field strength.

This research exemplifies the types of equipment used in wireless connection testing and measurement. In this work, a measurement of network usability was desired, so commercial-grade equipment was selected as the measurement hardware which implemented an established standard (IEEE 802.11g). Had pure signal strength measurements been desired, based on the

research of others, an entirely different array of equipment would have been selected. A measurement of signal strength alone would allow better analysis of the effect obstructions have on RF propagation, but would ultimately be less useful to the end-user who desires to implement his own wireless network for communications.

2.2 Range and Penetration Ability from Frequency

One of the most important factors in a signal's usable range, the frequency used in a communications system typically lies anywhere from single-digit megahertz to tens of gigahertz. Proper selection of the frequency to use depends on the system's operational requirements and in cases where purpose-built equipment is not being designed, the availability of hardware which operates in the desired frequency range. Of primary concern when selecting a frequency are the desired range of the system, the needed data throughput, and the penetration ability of the system. For these, frequency is directly related only to data throughput. An increase in frequency leads to both poorer range and poorer penetration ability of the signal for the same power.

The aforementioned studies utilized 2.4GHz communication for high-throughput ability systems. While 2.4GHz is a commonly used frequency for communications, other frequencies are commonly used for systems with different requirements. For example, Freeland et al. measured the effective range of real-time kinematic (RTK) location correction in mountainous terrain (R. S. Freeland, 2014). Since RTK operates in the 450MHz band, and is capped at 2 watts in the John Deere system used, the results of the paper show that 450MHz is a very capable choice of frequency for propagation through hilly and wooded terrain. The suggested maximum distance by Deere was 19km, with measurements being recorded out to 25km with approximately 50% of measurements providing useful RTK data at that distance.

By contrast, 2.4GHz is more easily defeated by obstructions to line-of-sight between transmitter and receiver. This is exemplified by Wu et al. in addition to many of the papers mentioned previously, which also used 2.4GHz was used to send data across farmland (H. Wu, 2015). Distances in these papers are typically measured in hundreds of meters, instead of kilometers. Wu et al. recorded RSSI measurements of 2.4GHz transmissions at using a spectrum analyzer out to 100m distance from the analyzer. They did this above and below the crop as well as at ground level. Even at these short distances, at 100m distance the received signal was often

below -110dBm in strength, which is unusable for most environments. These measurements were made with a transmit power of 4 dBm, or 0.0025 W, which is typical of nearly all 2.4GHz propagation studies.

2.3 Available Bandwidth from Frequency and Protocol Selection

In some cases, throughput capacity might take precedence over range in frequency selection. In this case, higher frequencies offer larger bandwidths, allowing more data to be sent. The Zigbee protocol used by Darr et al. and Wu et al. operates in the 2.4GHz band, and has a maximum bandwidth of 2MHz (M. J. Darr, 2008) (H. Wu, 2015). The Wi-Fi 802.11g protocol used in this work by comparison has a bandwidth of 20MHz, and is licensed to use up to 40MHz of bandwidth for data transfer. These large bandwidths are made possible by the 100MHz of RF spectrum allocated to the 2.4GHz ISM band between 2.4 GHz to 2.5 GHz.

On the 400Mhz band used by Freeland et al. (R. S. Freeland, 2014), users are restricted to a maximum bandwidth of 12.5 kHz called "wide band" or a maximum bandwidth of 6 kHz called "narrow band" depending on the user's license, in order to allow multiple users on the allotted frequencies between 450 MHz and 470 MHz. These smaller bandwidths greatly restrict the amount of data that can be sent wirelessly at these frequencies. This is the case because bands of radio spectrum at lower frequencies are divided into smaller sections based on the relative behavior of RF propagation at each frequency. Examples include high frequency signals (3 MHz to 30 MHz), very high frequency signals (30 MHz to 300 MHz), and ultra-high frequency signals (300 MHz to 3 GHz), which all behave similarly within their respective bands. It should be noted that as the bands climb in frequency, their overall bandwidth increases by an order of magnitude. Because of this there is less spectrum available for users at lower frequencies and so bandwidth restrictions are tightened. Thus, a tradeoff must be made when determining which frequency to use: throughput capacity versus range.

3. SYSTEMS

Many systems were designed and built to enable the collection of data during the project time frame. These varied from vehicle-borne wireless clients to wide-area Wi-Fi systems to board-level circuit design. This chapter is dedicated to the description of these systems, their technical specifications, and to provide an outline of the manner in which they interacted with each other. Specifically, these systems were the wide-area Wi-Fi network, the mobile sensor system, and the three stationary sensors. An overview will be given of each system's layout, constituents, and intended purpose. Following this will be a description of each component of the system, including relevant outstanding technical specifications and an overview of why each component was selected.

3.1 Wide-Area Wi-Fi Network

Design of the Wi-Fi network was largely derived from the projected needs of the system. The Throckmorton Purdue Agricultural Center covers an area approximately one mile wide and half a mile long. Thus, this was the area in which the wireless network needed to provide service. It was assumed that on a commercial farm there would be a grain elevator, large grain bin, or other tall structure on which an access point could be placed. Since TPAC was the home of the transmitter for WBAA, Lafayette's National Public Radio station, the broadcast tower located at the center of the research farm was used to simulate such a structure. This section will detail how the system was built, which components were used, and why each component was selected. The full bill of materials for the system is included in Appendix A.

As can be seen in Figure 3.1, the Wi-Fi system consisted of a sector antenna, a transceiver, a router, a server, two point to point link radios, and connecting ethernet cable. Every device that handled network traffic, with the exception of the server, was made by the hardware company Ubiquiti. As such, their browser-based configuration tool was used to adjust settings in each device. The settings used on each device can be found in Appendix B.
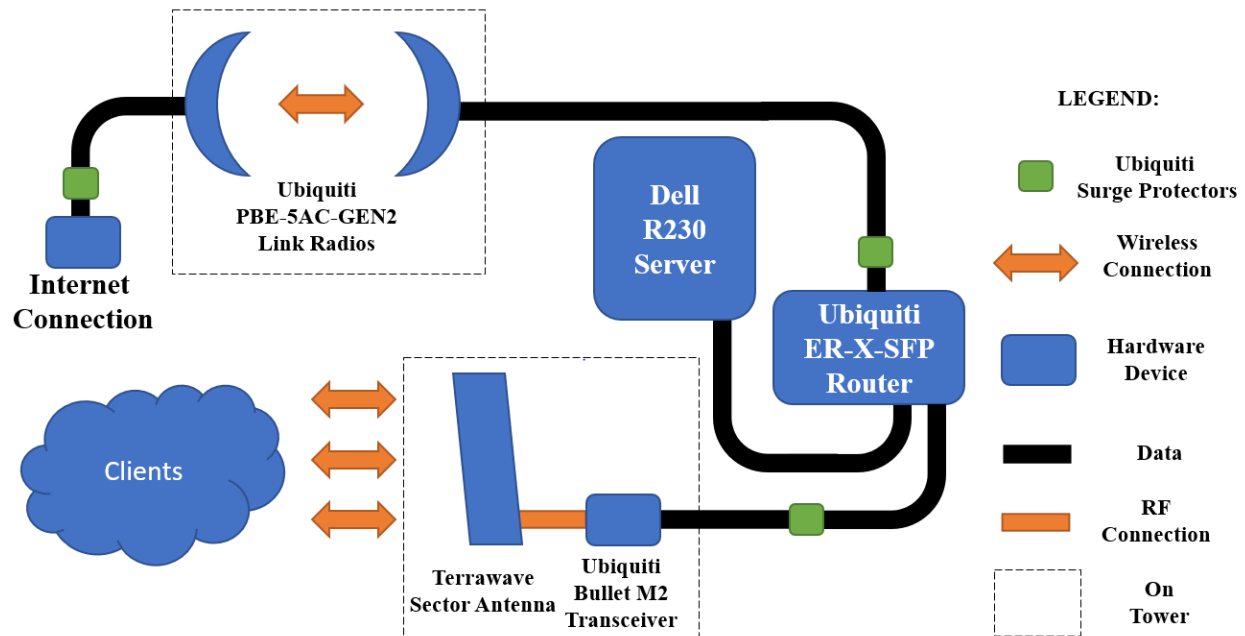
Figure 3.1: Diagram of Wi-Fi System

3.1.1 Access Point Antenna

Since the access point was to provide wireless coverage to the greatest area of interest possible, it was determined that antennas of the smallest possible beamwidth should be used to maximize the RF energy directed to the farthest reaches of the area of interest. This smaller beamwidth was determined to be 65⁰, and thus allowed higher gain antennas that to be used. Higher gain antennas could further project wireless signals and had a greater ability to receive signals in one direction with an improved signal to noise ratio when compared to antennas of lower gain or omnidirectional antennas. As can be seen in Figure 3.2, from the point of view of the broadcast tower, the furthest edge of the area of interest spanned 65⁰, so an antenna with corresponding horizontal beamwidth was chosen. The antenna chosen was the Terrawave T23180O10006-65X, referred to as "the Terrawave". The Terrawave antenna belonged to a family of antennas known as sector antennas, due to its intermediate beamwidth of 65⁰ between those of point-to-point antennae of extremely narrow

**Figure 3.2: Terrawave 65⁰ Degree
Antenna Coverage**

vertical and horizontal beamwidth and omnidirectional antennae, which radiate uniformly in the

horizontal plane. A special feature of the Terrawave antenna was that it could be connected to two transceivers simultaneously to cover two polarizations – ninety degrees offset from each other. This allowed for multiple-in-multiple-out (MIMO) operation, with two transceivers. The radiation pattern of the Terrawave can be seen in Figure 3.3. Since only one transceiver was being used, it was connected to the -45 degree feed port.
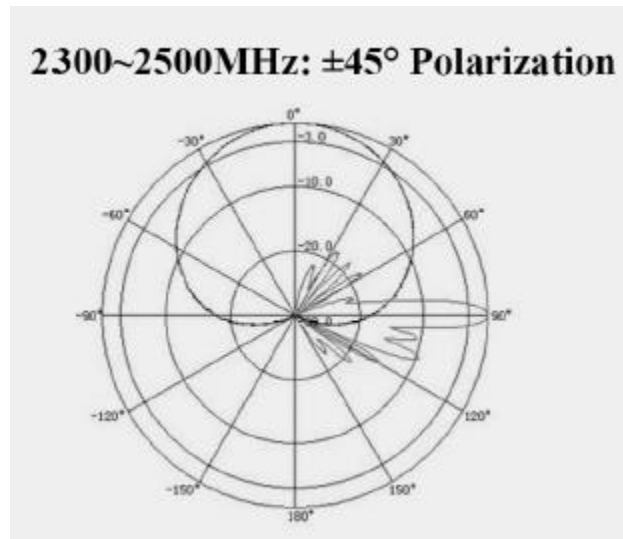
**Figure 3.3: Terrawave Radiation Pattern
(TerraWave Solutions Inc.)**
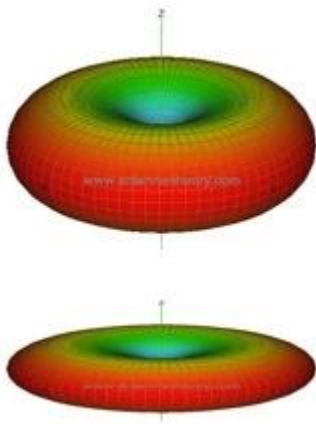
**Figure 3.4:
Low Gain (Top)
And High Gain (Bottom)
Radiation Patterns
(Hintersteiner, 2017)**

The Terrawave antenna was rated for a gain of 15dBi. This measure described the increase in radio frequency power in the intended direction due to the radiation characteristics of the antenna. This measure is easy to conceptualize using the law of conservation of energy. The same amount of energy provided to the feed point of an antenna must, ignoring all resistive and impedance mismatch losses, be radiated to the air in some direction. The greater an antenna's ability to focus this radiated energy to a single point, the greater its gain, as seen in Figure 3.4. For an antenna of high gain, the electromagnetic field strength in the direction of radiation would be high, but only for a small beamwidth, while for an antenna of low gain the electromagnetic field strength in the direction of radiation would

be lower, with a wide beamwidth. For high gain antennas this area of high radiated power could be dangerous to people or animals who cross its path, and as a result localized heating of tissues could occur, resulting in injury or death in extreme cases. Thus, the Federal Communications Commission (FCC) has placed restrictions on the strength of this field by limiting the effective

radiated power (ERP) of a system, measured in dBm. ERP can be found by adding the power input into an antenna, measured in dBm, and the antenna's gain, measured in dBi, is shown in the following formula:

Eq. 3.1
$$ERP = P_{in} + G$$

Where: ERP = Effective Radiated Power (dBm)

           P_{in} = Input Power (dBm)

           G = Antenna Gain (dBi)

According to the Code of Federal Regulations (CFR) 47 §15, this ERP from the Terrawave antenna is limited to 36dBm. Thus the input power need only be 15dBm at a perfect impedance match to meet this limit, which was easily attainable by the chosen transceiver. (United States Federal Communications Commission, 2019) Before installation, the impedance of the antenna was verified over the 2.4Ghz ISM band using a handheld network analyzer called a Field Fox made by Keysight. As shown in Figure 3.5, the antenna presented an acceptable standing wave radio (SWR) of 2 for the lower half of the 2.4Ghz ISM band. In the upper portion of the band, SWR climbed to nearly 4. Because of this, the access point was set to operate in the bottom half of the band.
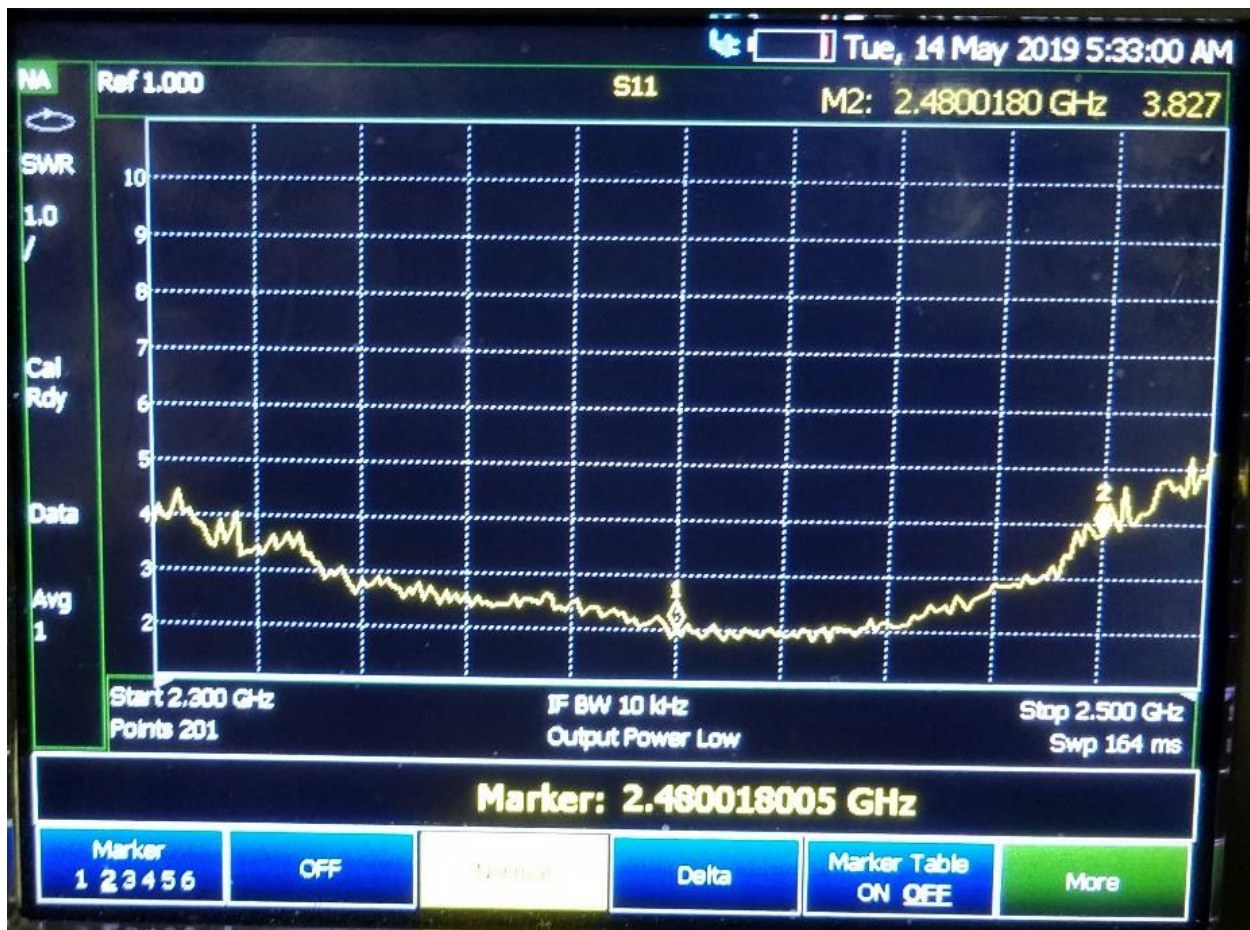
Figure 3.5: Standing Wave Ratio for Access Point Antenna

A tower climber was hired to perform the installation of the access point antenna and mated transceiver. During installation, the 9kW broadcast FM transmitter could not be deactivated, so the tower-mounted equipment was limited to the bottom of the tower to prevent excess RF exposure to the tower climber. As the tower was assembled in segments of six meters, and many mounting points were available at the 24-meter mark, the access point was installed at 24m (80') above the ground. This was also a common height for grain legs that would be found on commercial farms. Because of this, it could be assumed that radiation characteristics of the access point at 24m (80') would be like those of an access point mounted at the same height on a grain leg. Figure 3.6 shows the installation of the access point on the WBAA broadcast tower.

Figure 3.6: Installation of the Access Point

3.1.2 Access Point Transceiver

A 2.4Ghz transceiver provides the RF needed at the Terrawave antenna to connect to clients. The Ubiquiti Bullet M2, referred to as "the Bullet", was chosen among many possible devices. The Bullet is widely available from many resellers and demonstrates use of commercially available hardware that also has plentiful support. At less than $80 per radio, the choice was cost effective. The primary reason for selecting the Bullet was that it had an integrated N-type coaxial connector used to mate to the Terrawave antenna as seen in Figure 3.7. Combined with its onboard routing capability and the ability to be powered by 24VDC over ethernet, the Bullet was effectively able to act as an ethernet-to-RF transducer. Because of this, only a single ethernet

cable was needed to provide data and power to the unit when in operation on the broadcast tower. Like all other modern Ubiquiti transceivers, the Bullet M2 was configurable over its ethernet connection via SSH or web browser, enabling future programming changes to be made. Additionally, potential problems could be remedied without the need to hire a tower climber to gain physical access to the unit.

Figure 3.7: Ubiquiti Bullet with N Connector (Ubiquiti Networks Inc., 2011)

The Bullet was connected to the Terrawave sector antenna, along with an intermediary gas tube isolator that was included with the Terrawave. A gas tube isolator is a protective device containing a small tube of gas through which a conductor runs connecting the input and output connections. In the event of a lightning strike, the gas inside the tube expands and bursts the capsule, severing the connection and protecting any attached device from damage. The unit was programmed to transmit at 18dBm, in accordance with FCC regulations.

3.1.3 Base Station Router

While the Bullet described above could be connected directly to the test server to provide communication between the server and wireless clients, other wireless devices were needed elsewhere in the system to provide an internet connection and to serve other users. Because of this need to connect multiple devices to the wired network, a router was used to expand the number of ports available on the network, to organize wired traffic between devices, and to provide power over ethernet (PoE) to wireless transceivers when necessary. The router with the needed capabilities selected to fill this role was the Ubiquiti Edge Router ER-X-SFP, referred to as "the Router".

The Router was selected for its compact size, ability to power devices with PoE on every port, its plethora of support availability, and its low price. Additionally, the Router supports

configuration via secure shell (SSH) connection or web browser, allowing changes to be made remotely without physical access to the Router.

3.1.4 Point-to-Point Wireless Bridges

While TPAC was one of the closest Purdue research farms to academic campus, it was still several miles away. When problems arose, as they inevitably were bound to, it could potentially be impractical or frustrating to drive to the site to fix the problem. Additionally, without an internet connection, there would be no way to know whether all systems were online in between site visits. Because of this, internet connectivity was brought to the system through the use of point-to-point wireless transceivers. These transceivers needed to have enough throughput capacity that they would not bottleneck the system in any way. Also, they needed to operate on a frequency other than that occupied by the access point to prevent interference between the two systems. Thus, the Ubiquiti PBE-5AC-GEN2 PowerBeam, called the "PowerBeam", was deployed.

The PowerBeam is an ultra-high gain directional antenna, coupled with a 5Ghz Wi-Fi transceiver. It is powered over ethernet with standard 24VDC PoE and is configurable via Ubiquiti's browser-based configuration utility. Under optimal conditions, a wireless link between two PowerBeam units can support up to one Gb/s of throughput. As shown above, these point to point links were used to provide an internet connection to the broadcast tower site from a fiber optic cable termination in another building. This internet connection enabled remote diagnostics, configuration, and data collection to be performed without a physical presence at the research farm.

3.1.5 Ethernet Cable

Since the access point was installed on a tower supporting a broadcast FM transmitter, every component in the system had to be able to withstand high levels of ambient RF and high intensity electrostatic discharges. Because of this, shielded ethernet cable was used. As
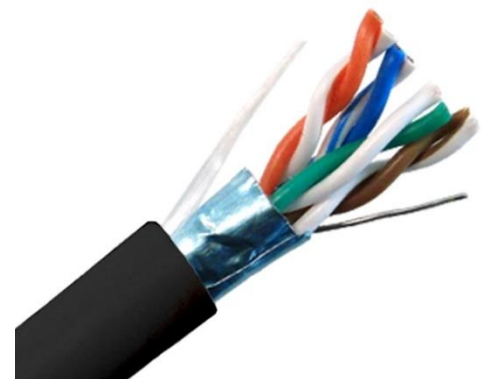
Figure 3.8: Shielded CAT6 Cable (Primus Cable, 2018)

26

shown in Figure 3.8, this ethernet had an additional layer of aluminum shielding containing all eight conductors, in addition to the usual ground wire. This shield layer acted as a local Faraday cage, preventing any outside RF from leaking into the cable, and it prevented parallel runs of ethernet from interfering with each other. Additionally, the selected ethernet was rated for outdoor use, which included a waterproof outer layer. These two characteristics of the cable enabled it to be used directly on the tower with no conduit or external shielding, allowing for easy installation and removal. As extended cable runs from the access point and point to point radios would be required, a spool of uncut ethernet cable was ordered and cables made at custom lengths. CAT6 ethernet was used due to its superior speed and signal isolation over CAT5e cable.

3.1.6 Ethernet Surge Protectors

In the event of a direct lightning strike on the broadcast tower, current would be dissipated into the ground by the network of buried copper ground radials attached to the tower, as per Motorola's station grounding guide (Motorola Solutions, 2005). However, nearby strikes not dissipated through the metal frame of the tower could cause a sudden increase in ambient air charge, leading to the formation of currents within any grounded metal object nearby. These currents could flow through the ground shield of the ethernet cable on the tower and into the systems connected on the ground. Because of this, it was necessary to install grounding points inline through which this charge could dissipate to ground.

A Ubiquiti ETH-SP was installed and worked by connecting the grounded shielding and the ground wire of the ethernet to the metal frame of the surge protector, which was then mounted to a grounded surface. It was capable of handling discharge currents of up to 5 kA, and it supported a data throughput of up to 1 Gb/s. Care was taken to only install one surge protector per device, as installation of multiple ground points within one run of ethernet could result in a ground loop, which would resonate and cause interference and data loss in the line.

3.1.7 Speed Reference Server

In order for data transfer to take place, there must be a sender and a receiver. Similarly, for network properties to be measured, there must be a client and a server between which data could be sent. In this system, there was a need for a computer that connections could be made to in order to test network properties. This computer had to have a network connection of great enough bandwidth (1 Gb/s) to not impose a bottleneck, it had to be capable of withstanding long periods of continuous uptime, and it had to fit within the physical space allocated for the project by the broadcast site manager.

To fulfill these requirements, the Dell R230 was selected. Designed as a server, its design intent included near-continuous uptime with a high speed ethernet connection and long-life hard drives. Ubuntu Server was installed on the machine because of its light weight, simplicity, and ability to run continuously for long periods of time without the need for a restart. Finally to respond to client requests for connection, the program iperf3 (McMahon, 2018) was installed and run in server mode.

3.2 Mobile Client

A mobile client was installed in a New Holland T8050 tractor and utilized to take wireless network measurements as the vehicle traversed a consistent route in the area of interest. Many components of the system were shared between the stationary clients and the wide-area Wi-Fi system, for the sake of simplicity. When applicable these previously mentioned components have been listed and their function described. A system diagram is shown in Figure 3.9. The constituents of the system are a transceiver, an RF switch to toggle between antennae, a high gain antenna, a low gain antenna, a GPS unit, a computer to act as a client and to execute network measurements, and the connecting coaxial and ethernet cables.
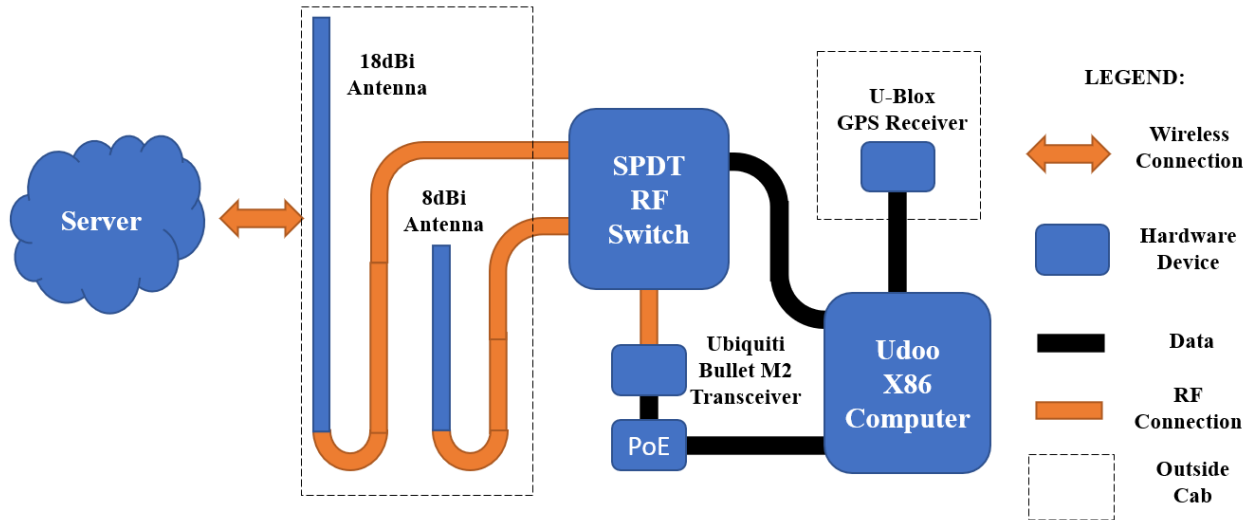
Figure 3.9: Diagram of the Mobile Client System

3.2.1 GPS Unit

To observe changes in network properties with changes in position, each measurement taken by the mobile client was tagged with GPS coordinates. To accomplish this task, an external GPS receiver was used that communicated via USB-A interface. The GPS selected used the U-Blox 7 chipset and was mounted on top of the tractor cab. Initial testing indicated that the accuracy of this GPS setup was confined approximately to a three-meter radius when using the wide area augmentation system, or WAAS, to improve the accuracy of GPS measurements.

Measurements of the GPS unit's precision were performed before and after the experiment by allowing it to run in a stationary location and collecting position measurements. Measurements were performed midday at each reading. For the purposes of verification, the unit was used to collect 50 location measurements for analysis. The primary concern that warranted measuring the precision of the GPS was that it would not provide a reading within the wheel base of the tractor, which was 3m. Thus, any standard deviation of less than 1.5m would be acceptable, indicating that 95% of readings would fall within the wheelbase of the tractor when the GPS receiver was centrally located on the cab. Figure 3.10 shows the coordinate span of the initial test, while Figure 3.11 shows the variation in altitude read by the GPS over the initial 50-reading test. Standard deviations for latitude and longitude were 1.14 m (3.74 ft) and 1.62 m (5.31 ft) respectively. The average of these was 1.38 m (4.525 ft), which was taken to be the

overall standard deviation of the unit. In the fall after all measurements were complete, the GPS was again tested for its precision using the same method. Figure 3.12 shows the result of the latitude-longitude post-season test, and Figure 3.13 shows the result of the longitude-altitude post-season test. In this instance, the GPS maintained a standard deviation of 0.25m (0.8 ft). Since all readings showed the GPS had a standard deviation of less than 1.5m, there was 95% confidence that all readings would land within the wheelbase of the tractor.
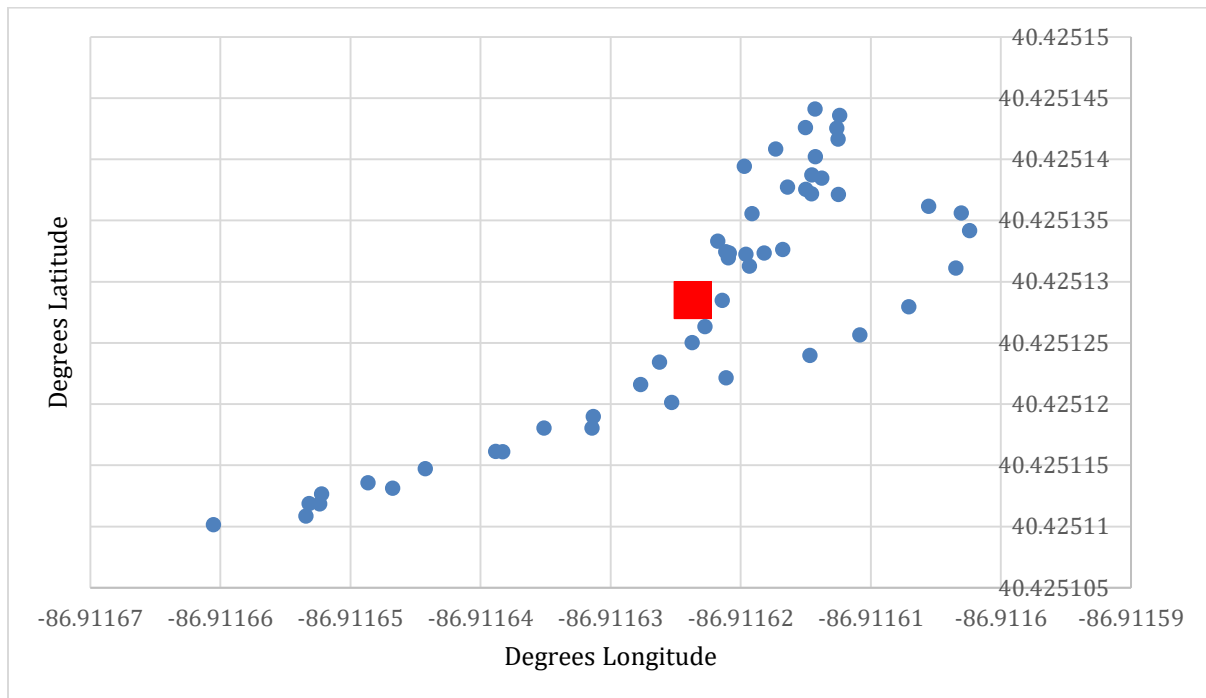
**Figure 3.10: Record of GPS Validation – Latitude vs Longitude
for Pre-Season (Red Square Denotes Group Average)**
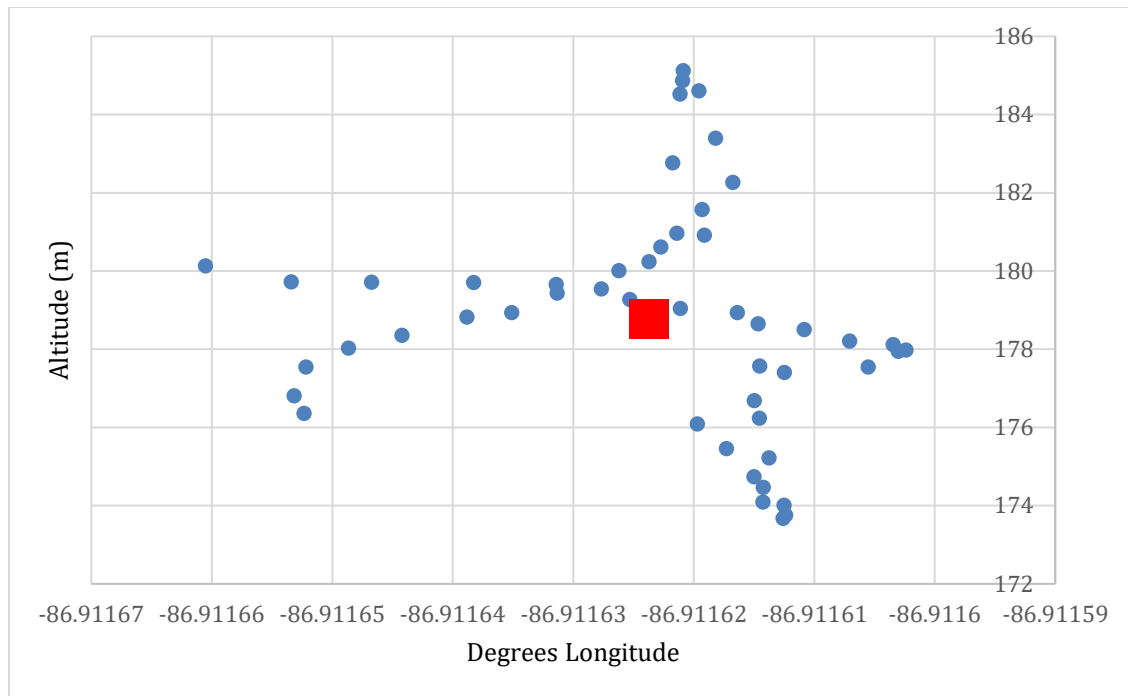
**Figure 3.11: Record of GPS Validation – Altitude vs Longitude
for Pre-Season (Red Square Denotes Group Average)**
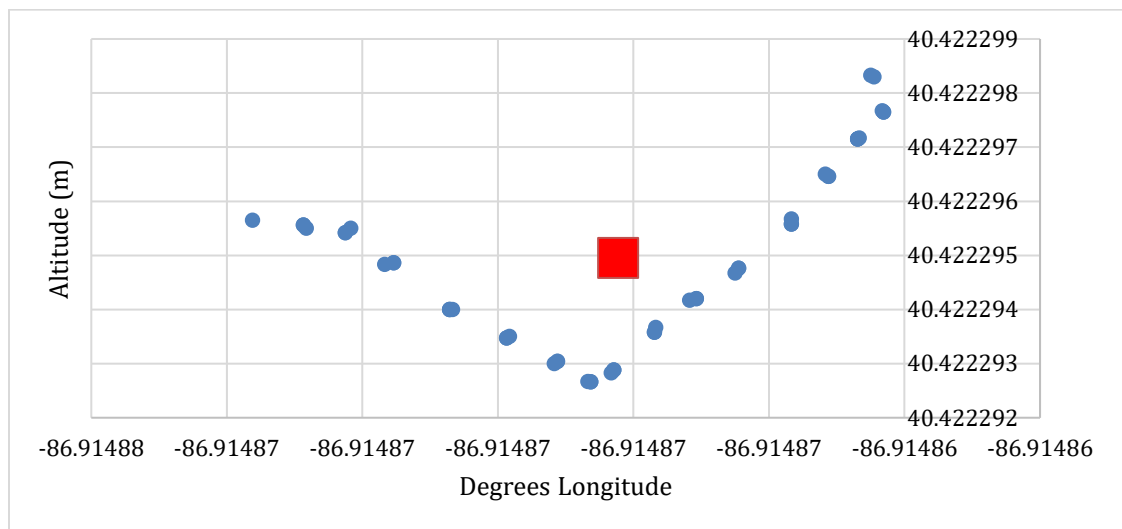
**Figure 3.12: Record of GPS Validation – Latitude vs Longitude
for Post-Season (Red Square Denotes Group Average)**

**Figure 3.13: Record of GPS Validation – Altitude vs Longitude
for Post-Season (Red Square Denotes Group Average)**
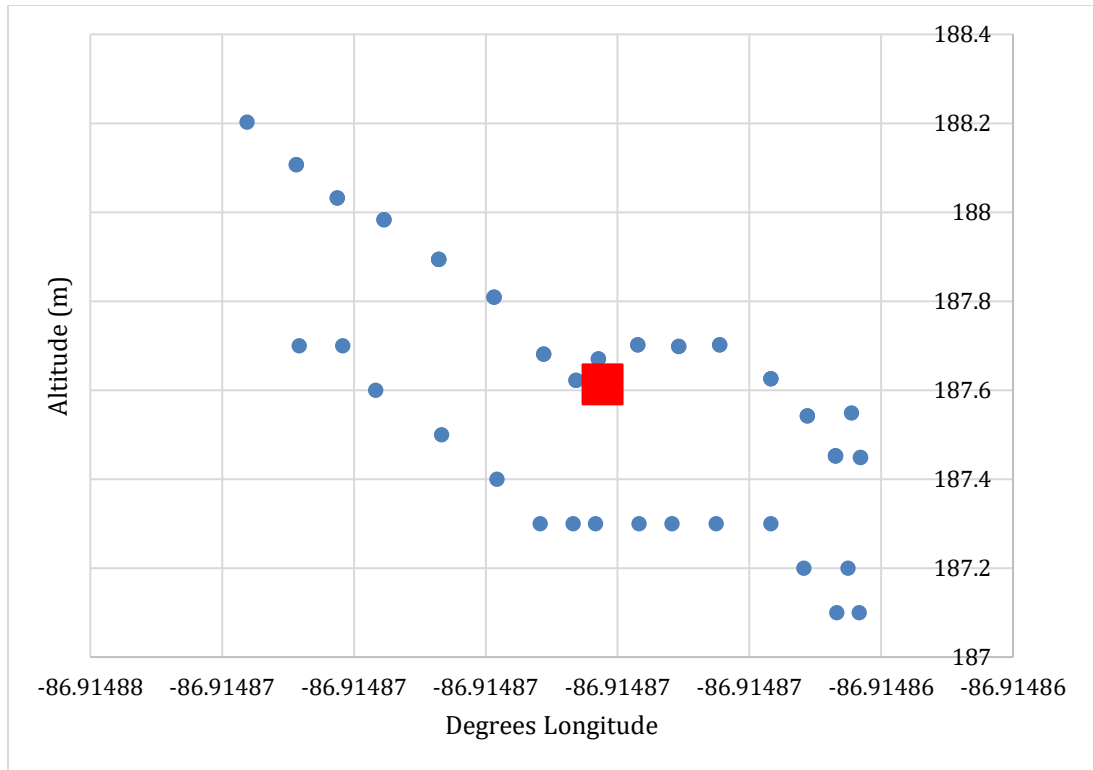
3.2.2 Data Collection Computer

Just as the server in the wide-area Wi-Fi system provided a connection endpoint for network testing, a computer was used to initiate network testing in the mobile client. The computer needed to have the capability to connect to the Bullet for Wi-Fi access, it needed to have a sufficiently fast wired connection to prevent a bottleneck, and it needed to be able to run the program iperf3 (McMahon, 2018) connecting to the iperf3 server. Initially, a Raspberry Pi 3 B+ was considered, but it has an insufficient maximum ethernet throughput of 300 Mb/s (Raspberry Pi Foundation, 2012) .

An Udoo x86, hereafter referred to as the "Udoo" (Seco SPA, 2018) was used as a computer capable of handling 1 Gb/s of network throughput. Linux Mint, a fork of the popular Linux distribution Ubuntu, was installed in the onboard storage, as well as the program iperf3, which could be run in client mode to connect to the iperf3 server to perform network characteristic measurements. Because of the programmable input and output (I/O) pins on the

32

Udoo, it was able to interface with the RF switch and control its actuation from the same Python script used to run iperf3.

Often shortened to "iperf", Iperf 3 is a command-line tool used to connect devices to a remote server also running iperf. Once connected to the server, iperf begins sending a set of packets known to both the server and the client. The user can configure this transfer of information in a number of ways, including the number of packets sent, setting the time it takes to complete a test, and determining if the test uses a UDP or a TCP connection. The iperf3 program ran as a terminal command and printed results to the shell. For the purposes of the project, this data needed to be recorded to a file. The Python script therefore issued the iperf3 command to the computer's shell and then parsed the output to the terminal for the desired information storage. After each round of measurement and data collection, the script also issued a command to the general purpose in-out (GPIO) header to which the RF switch was connected. This instructed the switch to toggle. This information was then stored and geotagged for later processing. The Python program used to control the switch and collect data can be found in the online repository at https://github.com/thiemep/TPAC-Wifi .

3.2.3 High Gain Antenna

High gain antennas were used to study their effectiveness at long range and in varying terrain. Due to the large nature of high gain antennas, they are rarely used on mobile equipment as they are prone to impact damage. For the purposes of this project, a high gain but sturdy antenna was chosen, the Hawking HAP15SIP. At 15dBi of gain, the omnidirectional antenna had a very narrow vertical beamwidth as shown in Figure 3.4. It was mounted on top of the tractor cab, as shown in Figure 3.14. By mounting the antenna above the roof line of the cab, it was assumed that the flat metallic surface near the antenna provided by the roof of the cab would act as a sufficient ground plane for the antenna.

8 dBi antenna

15 dBi Antenna

Figure 3.14: Mounted High-Gain Mobile Antenna

The antenna was mounted using a custom bracket and secured to the right-side mirror mount on the cab. The bracket allowed the antenna base to clear the top of the cab, avoiding any signal shadowing that could occur from an obstruction like the cab frame. The top of the high gain antenna was the tallest point on the machine at 5.4m (17' 8"). The antenna had to be removed when on the road to meet the DOT maximum clearance restriction of 4.3m (14'), and it also might be impractical amidst power lines, trees, and other obstacles.

3.2.4 Low Gain Antenna

Like the high gain antenna, the low gain antenna was used to study the effectiveness of a lower gain antenna at long range and with varying terrain. Being shorter than the high-gain antenna, the low-gain antenna was a more realistic application of a cab-mounted 2.4Ghz antenna, as it was less likely to impact low-clearance obstacles, and it fell under the DOT road height restriction of 4.3m (14'). For this role, the C. Crane 8DB was chosen. The antenna had an

omnidirectional gain of 8dBi, just over half of the 15dBi of gain provided by the high-gain antenna. It was hoped that this antenna would be less susceptible to changes in terrain, due to its wider vertical beamwidth, as shown in Figure 3.4. Unfortunately, it was predicted that at longer distances this antenna would be less able to maintain a reliable connection to the access point, because of its relative lack of directivity. The testing within this research program was designed to test this hypothesis.

3.2.5 Coaxial Cable

To allow the transceiver and RF switch to be located inside the cab and out of the weather, coaxial cable was used to transfer RF energy from the transceiver to the switch and from the switch to the two antennae mounted on the roof. As RF energy transmitted through coaxial cable increases in frequency, the energy loss per unit length increases exponentially. This can be seen in the loss chart in Figure 3.15. This is the reason that for microwave frequencies and above, waveguides are typically used, as they present lower losses per unit length when tuned for a certain frequency. Since a rigid waveguide would be impractical, and the coax runs were only 3m (10') long, the lowest loss coaxial cable practical was selected, which was LMR400. (Chew, 1990)

LMR400 coaxial cable is a recent development of Times Microwave superseding the older RG-8 size coaxial cable. LMR400 presents a 50-ohm impedance, which the Bullet and antennas were designed to use. Because of this, no matching network was necessary to use LMR400 cable. Additionally, LMR400 was rated for outdoor use. It was waterproof, UV resistant, and rated for direct burial, making it ideal for use outside the tractor's cab. While its center conductor was solid, its rated minimum bend radius was four inches, which was acceptable for installation on the tractor cab.

Coaxial Cable Choices for antennas.us products
Attenuation per foot length of cable as a function of frequency
Frequency range of 0.1 GHz to 26 GHz
Property of Myers Engineering International, Inc. (C) 2008

antennas.us Coaxial Cable Choices
- RG-316
- RG-142
- RG-405
- RG-402
- LMR-195
- LMR-400
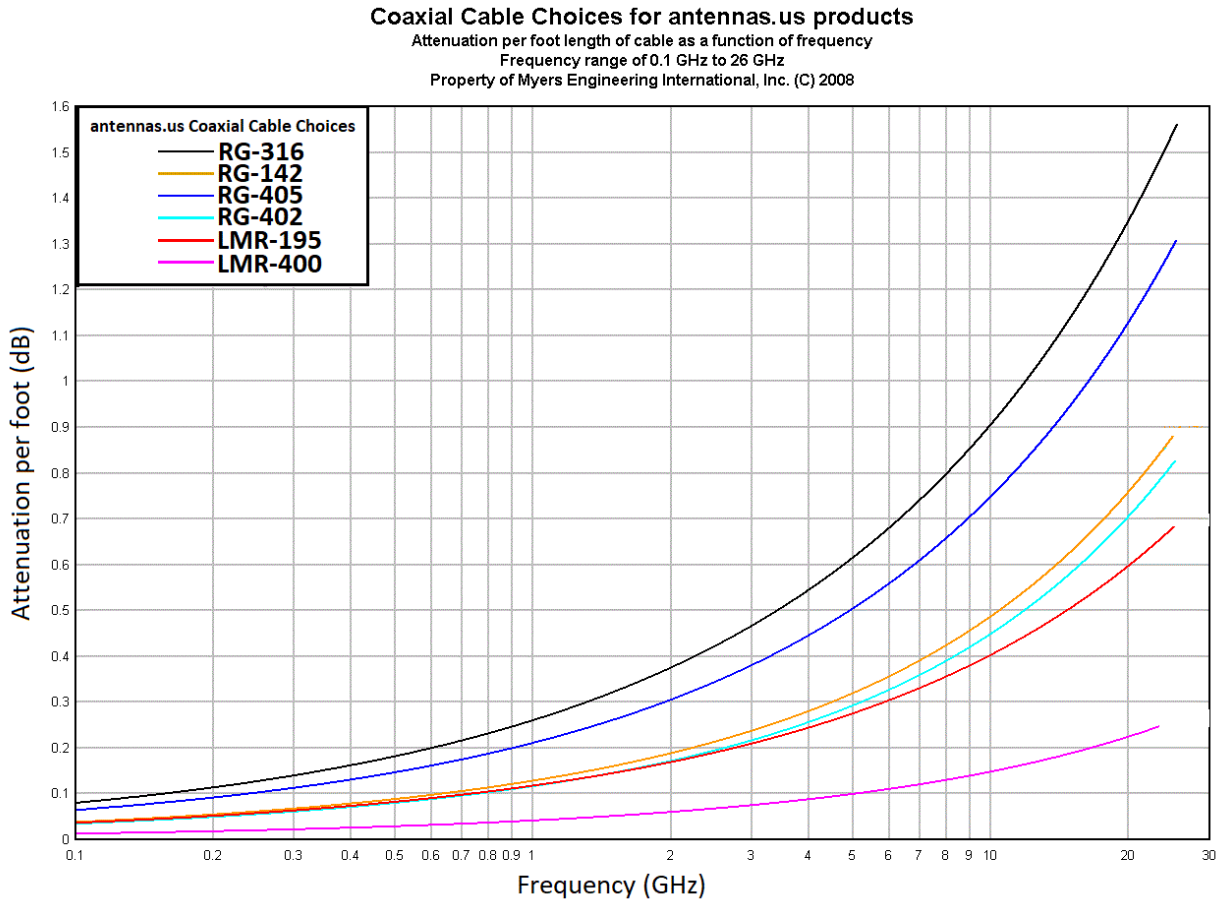
**Figure 3.15: Attenuation per Length of Coaxial Cable
(Myers Engineering, 2008)**

3.2.6 RF Switch

The only piece of custom hardware used in the project was the RF switch that enabled sequential network measurements between the high gain and low gain antennae. A single pole double throw, or SPDT, switch was needed to allow one transceiver to connect to two antennae. A General Microwave model G9120-3-9-27 fit the needs of the project, but it cost $2,250 per unit, so a custom solution was designed.

The switch board was designed by consultant Ahner Engineering and is illustrated in Figure 3.16. The switch was designed to use SMA-type RF connectors and was controlled by a four-pin header providing power, ground, control, and logic switching lines. Coplanar waveguides were used to carry the signal to and from a switching integrated circuit (IC), with

36

matching networks made from surface mount components on each length of waveguide. After installation, the switch was swept with a handheld network analyzer to ensure that it presented a 50 Ohm impedance to the transceiver and that there was sufficient isolation between the two antenna ports to ensure than no leakage between them. The actual RF switch used is shown in Figure 3.17. The final cost was $200 per switch.
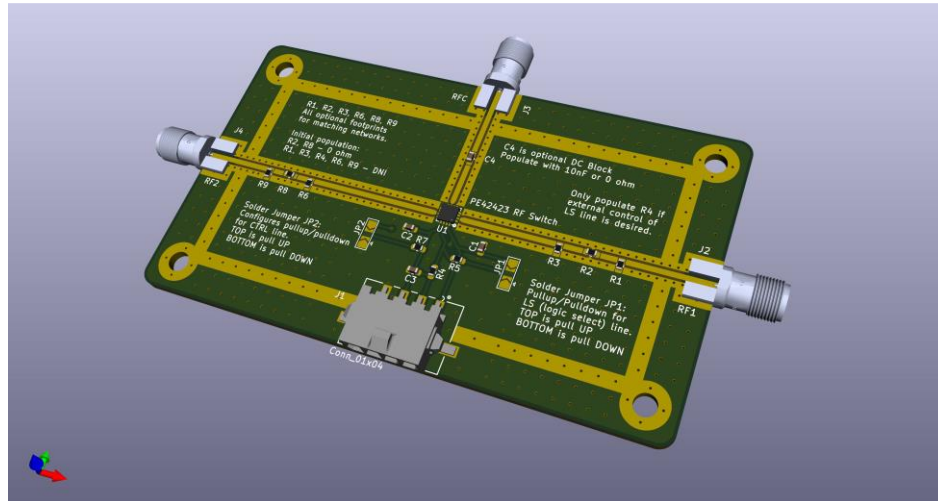
Figure 3.16: CAD Model of SPDT 2.4GHz RF Switch
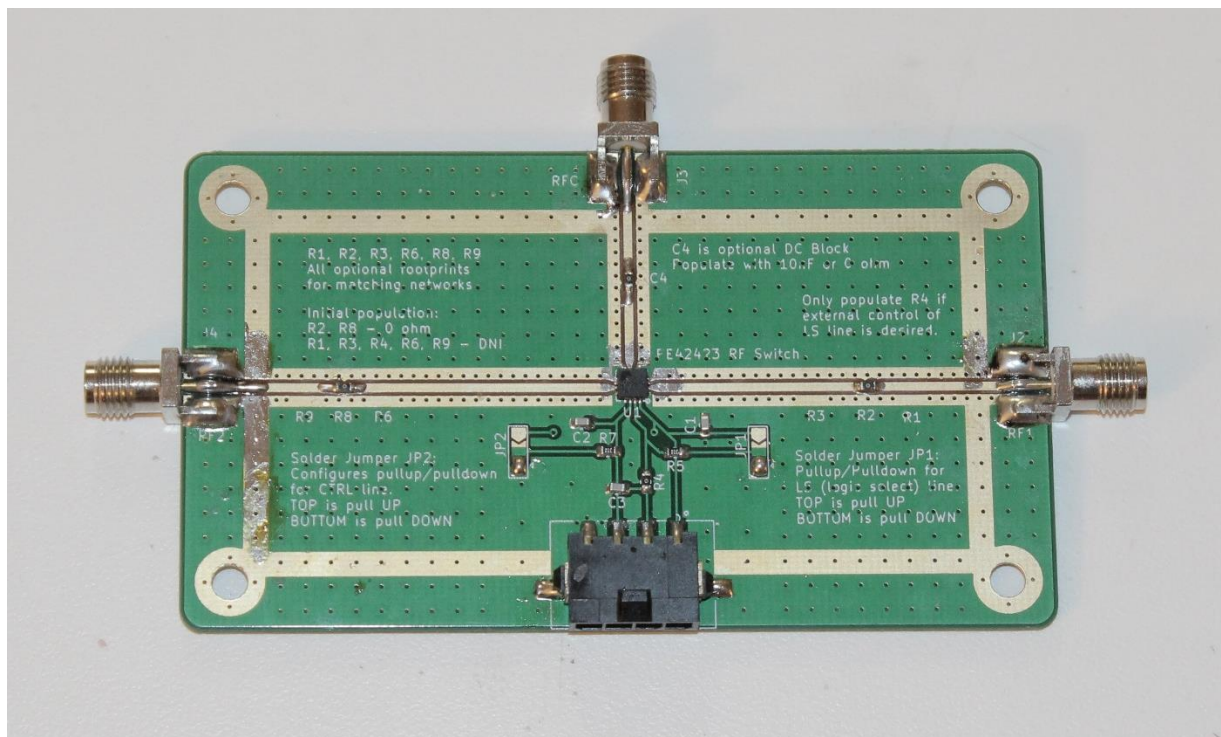
Figure 3.17: SPDT 2.4GHz RF Switch

The measurements of standing wave ratio (SWR) for high and low gain antennas through the switch, as well as antenna isolation measurements, can be seen in Figures 3.18, 3.19, and 3.20, respectively. SWR measurements were made using a vector network analyzer (VNA) made by Keysight called the Field Fox (Keysight Technologies, 2018).

The Field Fox in network analyzer mode was calibrated using the supplied open, short, and 50-ohm terminations. Briefly, a VNA measures RF characteristics of a system by injecting calibrated RF signals into the device being measured through one port and then measuring the phase and amplitude of the returned signal. This returned signal can be measured on the same port as the original signal was emitted from, called an S11 measurement, or it could be measured from a different port, called an S12 measurement. In these examples, the first number in the "S" signifier is the port from which the signal originates, and the second number in the signifier is the port on which the returned signal is received. Hence, an S11 measurement is used to measure reflection, and an S12 measurement is used to measure loss.

The device to be measured was connected to port one, and an S11 measurement taken. The S11 measurement was the measurement of reflected power on port 1, relative to the power output by port 1. By measuring returned power from an antenna, its efficiency as a radiator of RF energy can be measured. By the law of conservation of energy, all energy fed to the antenna must either be transmitted to the air, dissipated as heat, or returned to the source. Since resistive heating is extremely minimal in a properly constructed system, it was assumed that any power not returned to the source was transmitted to the air. Thus, the frequencies on the S11 measurement that show the lowest returned energy were said to be the most efficient frequencies at which the antenna would radiate. This relationship between input power (also called forward power), reflected power, and SWR is shown by:

Eq. 3.2
$$SWR = \left(\frac{1 + \sqrt{\frac{P_r}{P_f}}}{1 - \sqrt{\frac{P_r}{P_f}}}\right)$$

Where: SWR = Standing Wave Ratio (unitless)

                P_r = Power Reflected from the Antenna (dBm)

                P_f = Power Forward to the Antenna (dBm)

In Figures 3.18 and 3.19, the edges of the 2.4Ghz ISM band are marked by markers 1 and 2 for the lower and upper portions of the band, respectively. Both antennas were measured to have SWR measurements of under 2 for the entire 2.4Ghz ISM band.

Once the SWR was measured and it was determined that adjustment of the matching networks on the switch was not needed, the isolation between the transceiver and the inactive antenna port was measured. This was a critical statistic to measure, as any signal leaking through the switch from the unused antenna would distort the results of any network testing done. Since the two antennae were tuned to resonate on the same frequency band and were located to close to each other, any transmission made by one antenna could potentially be heard by the other very strongly. This was the RF equivalent of standing too close to a speaker at a rock concert. To prevent this signal in the unused antenna from reaching the transceiver, the RF switch can block signals up to a certain strength. This was known as the isolation capacity. In this instance, as shown in Figure 3.20, an S21 measurement was taken where a signal of -15dBm was injected into the unused antenna port and RF energy leaking through the switch was measured at the transceiver port. As shown in the chart, the signal that leaked through the switch had a strength of -40dBm, an attenuation of 25dB.
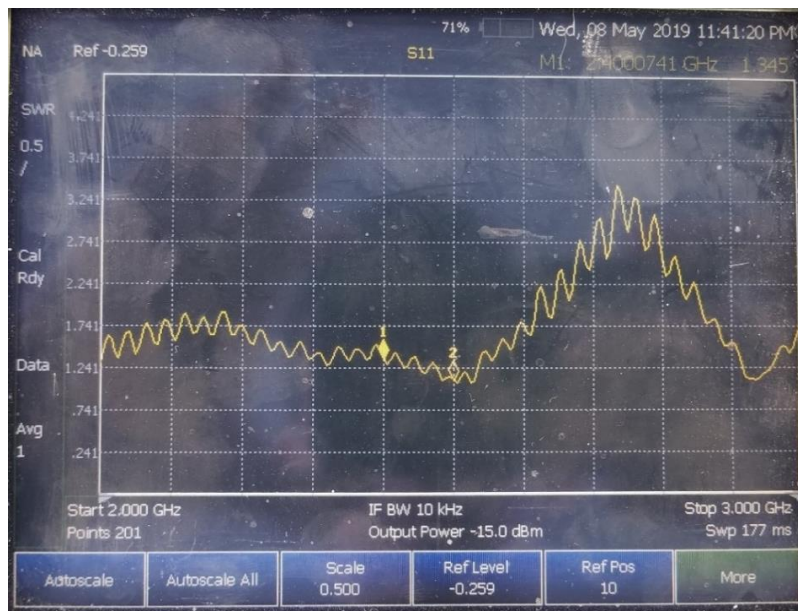
**Figure 3.18: Standing Wave Ratio of Low-Gain
Antenna Through RF Switch**
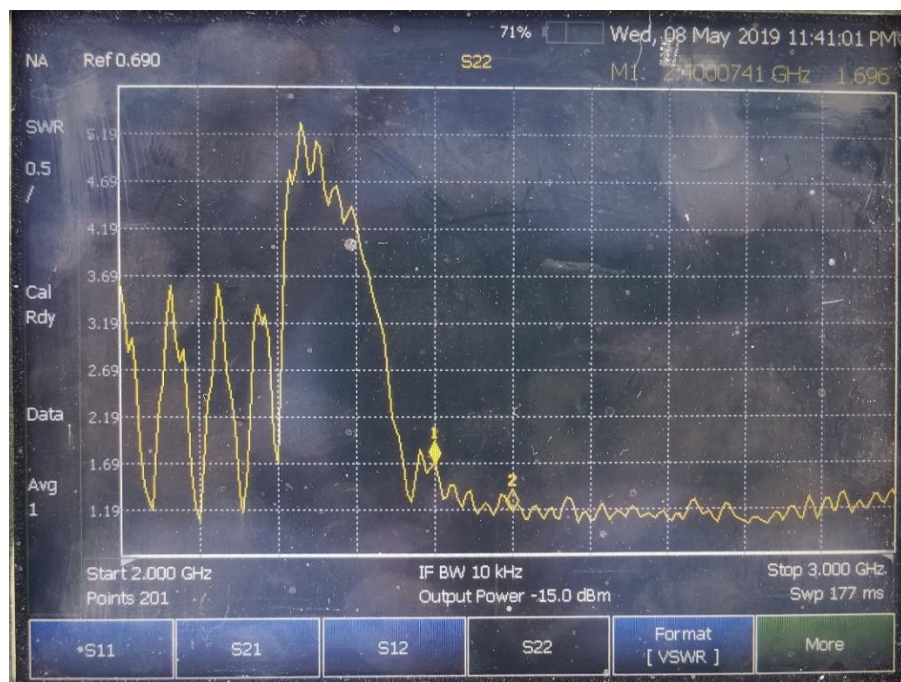
Since the maximum ERP seen on the roof of the tractor was from the high gain antenna at 36dBm (4 Watts), this was used to calculate the power seen by the transmitter as a result of leakage through the RF switch from the unused antenna. After free space path loss, the power seen at the switch was 23.4dBm, which after further attenuation by the switch itself, the power seen by the transmitter was -1.6dBm, this was approximately 0.0007W, or approximately $\frac{1}{5700}$ of the ERP emitted by the high gain antenna.
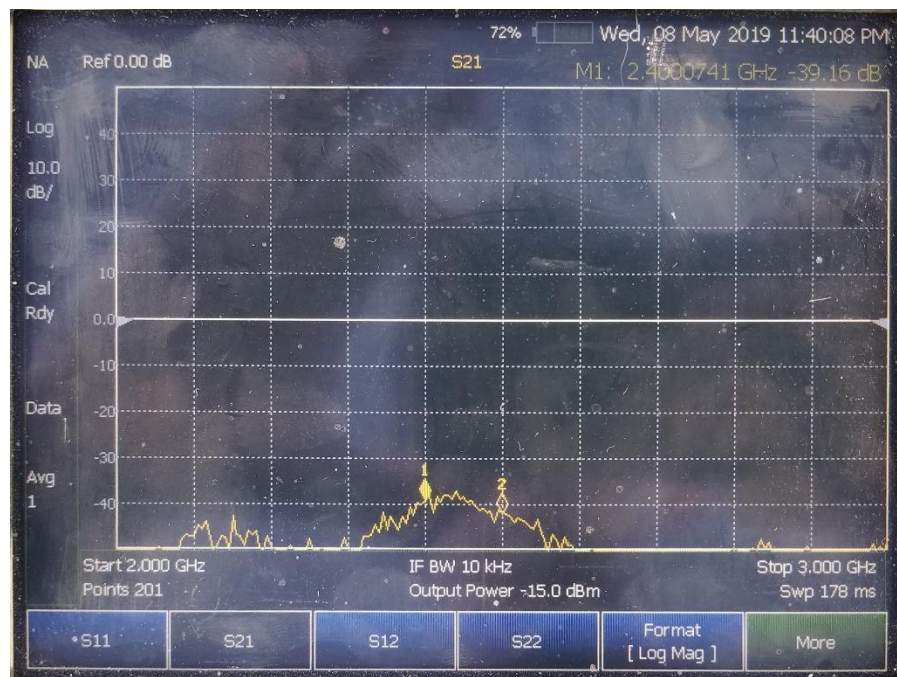
Figure 3.20: Isolation Between Antenna Connections

3.2.7 Ubiquiti Bullet

As in the wide-area Wi-Fi network, the Ubiquiti Bullet M2 was used as the transceiver in the mobile client. One of the reasons the Bullet was chosen for this task was its ability to act as both an access point or a client, depending on programming. As the Bullet used for the access point was programmed over ethernet, so the Bullet in the client machine was programmed over the network to automatically connect to the test network upon startup. However unlike the Bullet used as the access point, a constant power output level could not be specified. This was due to the use of two antennae of different gain levels, which emitted different ERPs at a given input power. As mentioned previously, the FCC mandates that the ERP of a system be below a set

41

threshold for a given frequency. For the Bullet to maintain the same ERP for both antennae, it would need to alter its power level depending upon which antenna it was connected to. This is a feature that the Bullet did not support. Therefore, to avoid violation of CFR 47 §15, the transmit power of the radio was capped at the power needed to achieve the maximum legal ERP of 36dBm on the high gain antenna of 15dBi, which was 21dBm of power transmitted from the radio. (United States Federal Communications Commission, 2019)

3.3 Stationary Sensor Systems

Similar to the mobile client, the stationary sensors took wireless network measurements at fixed distances along a radial line extending from the access point to the furthest point in the area of interest. Every component present in the stationary sensors was also present in the mobile client, except for a battery to power the sensor. A system diagram is shown in Figure 3.21. The constituents of the system are a transceiver, an antenna, a computer to act as a client and to execute network measurements, a battery to power the system, and connecting ethernet cables.
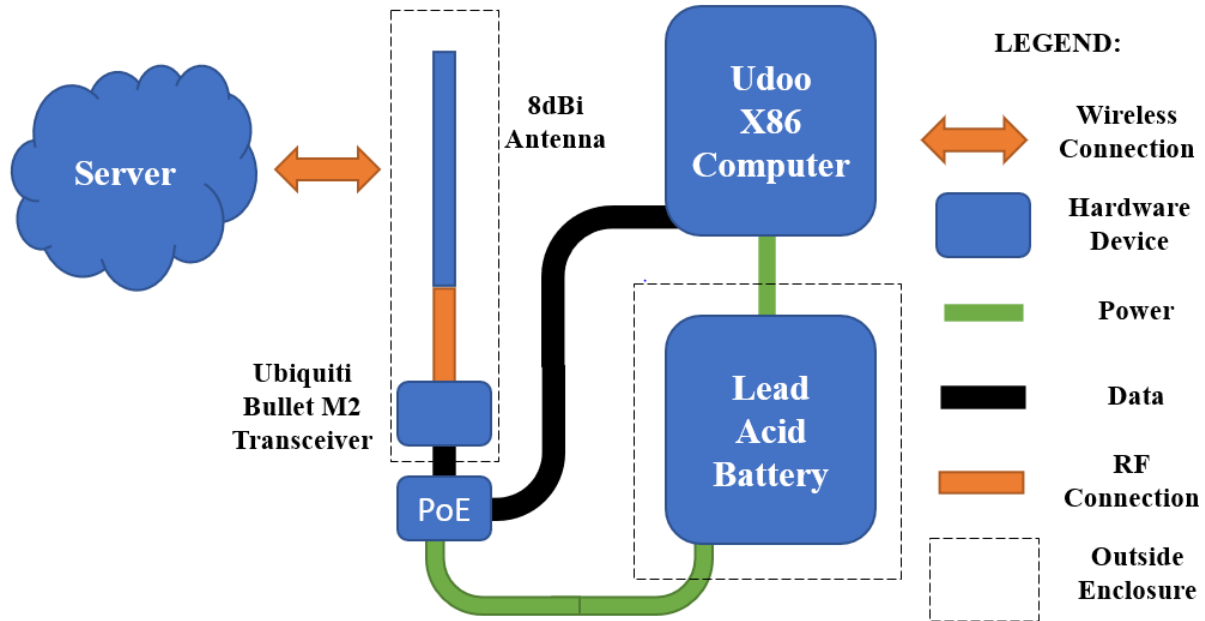
Figure 3.21: Stationary Sensor System Diagram

3.3.1 Housing and Fixturing

Since the stationary sensors were to be outside for the duration of the growing season, their water-sensitive electronic internals needed to be protected from wind, rain, and snow. To accomplish this, plastic National Electrical Manufacturers Association (NEMA) style water resistant enclosures were used. These housings included rubber gasketing around the enclosure door, which prevented moisture from seeping inside. The cases were also pre-creased with punch-out blanks to make holes in the box, if the end user required. Two of these punch-out blanks were removed in each box to allow space for power and data cables to be run through.

The boxes were suspended on t-posts to keep them off the ground. Not only did this prevent water or mud from entering the boxes, but it also discouraged any wildlife from attempting to gain entrance. Some 2.1m (7') t-posts were chosen as supports. Once driven into the soil, they provided a 2m (6') post on which to mount the antenna and visibility flag. In this way, all necessary devices could be mounted on one post, while the battery running each sensor could sit on the ground for easy replacement. Figure 3.22 shows a deployed field sensor.

3.3.2 Antenna

Unlike the mobile client, the sensors were equipped with a single antenna. This antenna was the C. Crane 8dBi antenna used as the low-gain antenna on the mobile client. These were mounted at a height of 2m (6') above the ground, atop the t-post that supported

Figure 3.22: A Deployed Field Sensor

the sensor electronics. The FCC mandated ERP limit of 36dBm was met by limiting the input power to the antenna, which was 28dBm. It was assumed that the antenna would behave in the same way as the other 8dBi antennae that were used, similar to the SWR measured in Figure 3.18. Because of this, it was assumed that there was as good impedance match and that the losses due to mismatch and to resistance were negligible.

3.3.3 Battery

Permanent or semi-permanent field sensors are seeing an increased use to gather field data, and with their increasing deployment, new and innovative ways of powering them have been developed. However for this project, the goal was to measure network characteristics over a growing season and not to develop new ways to power field sensors. Deep cycle marine batteries were used to run the sensors. For three sensors, six batteries were purchased so that one set would be running the three deployed sensors, while the other was charging. Run time on one battery was measured at just over 1 week, with full uptime of the Udoo computer and the Bullet transceiver. The batteries used were DC27HDT deep cycle 12V marine batteries, with a reserve capacity of 182 minutes.

4. METHODOLOGY

4.1 Overview

Several approaches could be taken to measure the viability of a microwave-based system for data transfer. One could simulate the environment in software such as Dassault Systems' CST using LIDAR data taken of the area, and then use this simulation to model projected propagation characteristics based solely upon Maxwell's equations. Similarly, one could measure the attenuation of various obstacles like crops, trees, and buildings, and then use the resultant data to predict what the total attenuation would be from several of these obstacles as they might be arranged at a location of interest.

While these methods may provide insight into the projected propagation characteristics of microwave radiation, there are many variables that would need to be taken into account to yield a realistic model. How will the obstacles change over time? How will weather affect the transmission of signals? Are the ground planes presented by agricultural equipment sufficient to support an antenna of sufficient gain to transfer data at the desired distance? To give an accurate model, many such questions would need to be answered with ancillary research. Thus while analytic analysis would be possible, it was decided that a real-world experiment should be used to measure the actual capability of such a system, instead of attempting to describe its characteristics mathematically.

Since the purpose of the experiment was to measure the functionality of the system, the two most common users of such a system were utilized to measure its capabilities, a mobile client and stationary clients. These were constructed to be as similar to what an in-field product might be as possible. Sensors were placed at regular distances from the access point to measure the effect of distance on throughput and latency. A tractor was used to carry the mobile client, since it was the most common mobile platform in the field. Since the goal of the experiment was to cover a dedicated area, a directional antenna was used at the access point to provide the most comprehensive coverage of the area of interest given a single access point.

Wi-Fi connections send data by dividing the information to be transmitted into small divisions called "packets". These digital packets are sent by one party and received by another in serial fashion until all data has been sent. This project used modern 2.4Ghz Wi-Fi equipment

capable of sending data according to the 802.11 b, 802.11 g, and 802.11 n standards. 802.11n was the most recent of these, and supported multiple-in multiple-out (MIMO) transmissions. In this scheme, multiple receivers and multiple transmitters work simultaneously, increasing available bandwidth and decreasing errors in packet reception. For MIMO to operate, antennae intended for MIMO use must be used as they must connect to many transceivers. MIMO was not used for the sake of simplicity, and the transceivers were programmed to operate under the 802.11g standard which only used one antenna per transceiver. (Sharony, 2006) (Ubiquiti Networks Inc., 2011)

Data transferred under the 802.11g standard uses orthogonal frequency-division multiplexing (OFDM). OFDM, developed by Bell Labs in 1966, is a method of using multiple frequencies simultaneously in one transmitter to encode data and is one of the most widely used modulation schemes in Wi-Fi connections. Under the most favorable signal conditions, the 802.11g standard uses ODFM modulation to transmit data at up to 54 Mb/s. If signal conditions decrease to levels unable to support accurate decoding of ODFM data, the 802.11g standard can switch to a slower but more reliable modulation type, like complimentary code keying (CCK) at up to 11 Mb/s or differential phase shift keying (DPSK) at up to 2 Mb/s. These standards were previously used in 802.11 standards for wireless communications. (Dekleva, 2007) (Jangeun Jun, 2003)

Unfortunately, the Bullet M2 does not export the data it receives about signal strength or environmental RF conditions. Therefore, the measure of signal integrity between clients and the access point had to be measured with other metrics. Network properties were selected to be the characteristics used to determine the usability of a connection. These properties were throughput capacity in Mb/s, network latency in milliseconds, and the number of data packets dropped within a specified interval. Measurements of these characteristics were taken by use of transmission control protocol (TCP) and user datagram protocol (UDP) connections.

TCP and UDP were protocols used on top of the internet protocol (IP) layer, which was responsible for managing connections between computers on a network. For the purposes of this project, it was not necessary to provide a comprehensive explanation of how TCP and UDP operated, but the relevant characteristics of each protocol are as follows: TCP had integrated error checking for increased data transfer reliability. It was the primary protocol used when accessing webpages and transferring files between computers. UDP was a protocol that

46

emphasized decreased latency between computers across a network, and as such did not handshake with the target before data transmission or have any integrated error checking as TCP did. Since the two protocols emphasized corrected data transfer and low latency respectively, they could be used in conjunction to measure network properties and to determine the health or usability of the connection. (Jangeun Jun, 2003)

4.2 Mobile Data Collection

To directly measure these network properties in an agricultural setting, a client and an access point were used. A 2.4Ghz access point was placed on a nearby elevated structure so that it had line-of-sight to a specified area of interest, and then it was connected to a server. To simulate usage on a farm, a tractor was fitted with a 2.4Ghz Wi-Fi radio, an onboard computer, and external antennae. When the tractor's radio was locked to the access point, and data was sent from the onboard computer to the server, the aforementioned network properties could be measured. Further, the tractor was made to travel along a predetermined route in the area of interest while these measurements were taking place. By referencing the recorded measurements with GPS data, a map of coverage could be created. This system, shown in its most basic form in Figure 4.1, was covered in detail in Section 3.
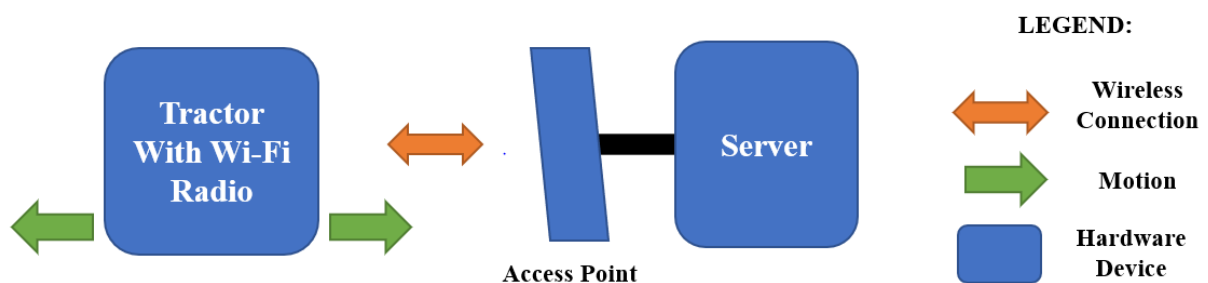
Figure 4.1: Mobile Client System for Network Properties Measurement

Radio signals are best received when there are no obstructions to the path of the wave. This is why wireless internet service providers (WISPs) in rural locations often use grain legs, grain bins, large buildings, or other tall objects to place their equipment. By locating the access point of a system on the tallest point possible, the greatest amount of area can be serviced. To

simulate this, the access point previously mentioned was placed on a radio tower at the Throckmorton Purdue Agricultural Center (TPAC). This tower was the only object of significant height at this farm and was centrally located on the property. Typically, a centrally located access point would be desirable, as it would provide a central point on which to place lower-powered access points. However in this instance, a centrally located access point was not desirable, as it limited the range at which measurements could be made.

A map of TPAC can be seen in Figure 4.2, highlighting its boundaries as well as the location of the tower and the area of interest. The central location of the tower greatly limited the selection of an area where the measurements could be made. Had the tower been located at the edge of the property, the longest radial distance from the tower would have been much greater, allowing wireless measurements to be taken from a much greater distance. Since the tower was centrally located, the south-westernmost quarter of the property was chosen as the area of interest, since it provided the longest line-of-sight distance available on the farm.
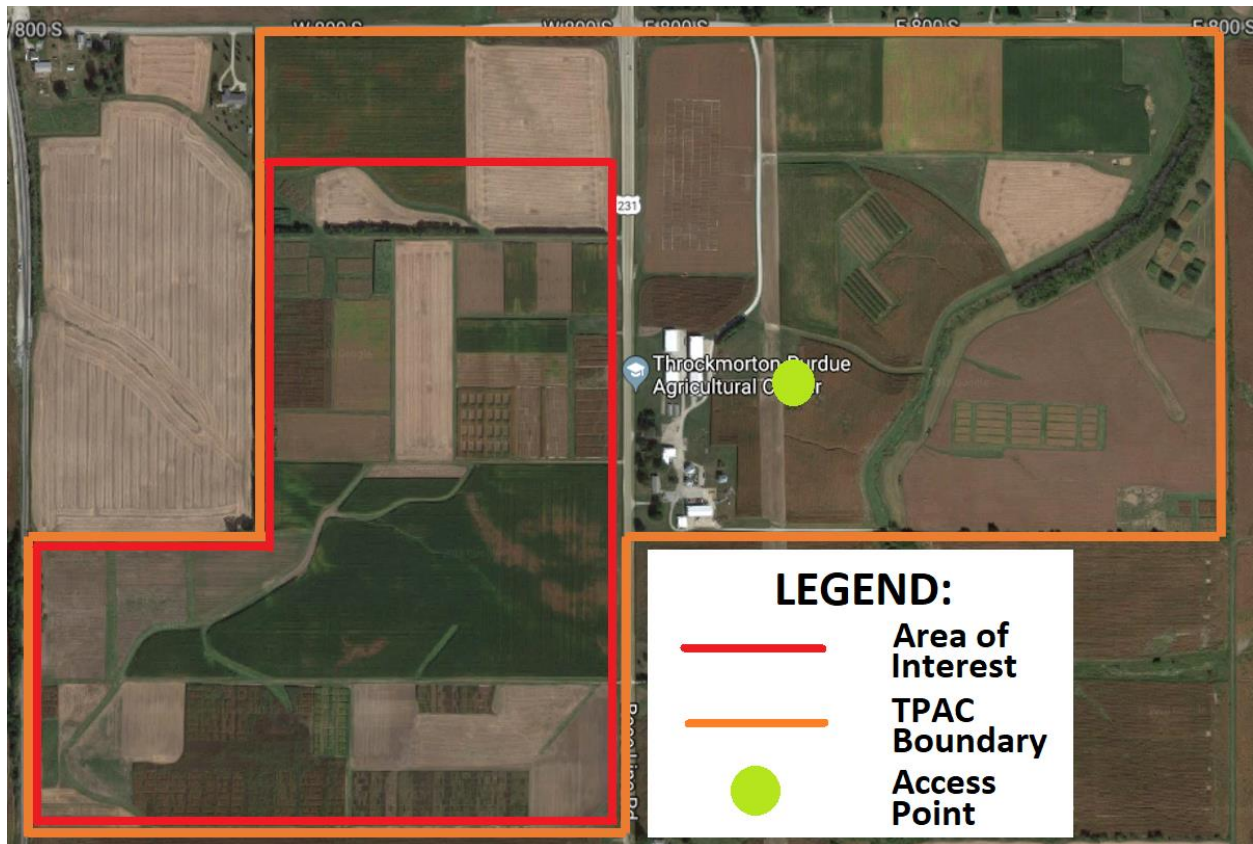
Figure 4.2: Boundaries of the Throckmorton Purdue Agricultural Center (TPAC)

To obtain the most useful georeferenced network properties possible, route planning for the tractor had to cover as much of the area of interest possible. Ideally, this would consist of arcs concentric with the access point at even intervals to obtain measurements at consistent distances for every angle of the access point's antenna. This homogenous sampling path would allow a heatmap to be constructed. However on a production farm where the three-dimensionality of crops is of vital importance, this was an impossible criteria to achieve. Instead, existing access paths and trails were exclusively used to plan the travel route and avoid any crop loss. The route was planned using the greatest number of grassed paths possible, including pathways close to and far from the access point, at the extreme edges of its area of coverage, and behind as many crops as possible to observe their effect on signal properties, if any. A visual of the path can be seen in yellow in Figure 4.3. As previously mentioned, TCP and UDP connections were used to make the network measurements. This was accomplished using Iperf 3.

TCP and UDP protocols were used in conjunction to collect connection properties. Using a TCP connection allowed the amount of throughput available to be measured, and the UDP connection provided the number of packets incorrectly received in a test of a set duration, as well as the latency of the connection to the server. By default, iperf ran the specified test until a certain amount of data was sent, at which time the test concluded. However, using the amount of data sent as a metric for the progress of the test made the test duration dependent on the connection speed. For a moving client that needed to perform network measurements at regular intervals, this was unacceptable. The test type was changed to a timed test of three seconds. At a typical inter-field transit speed of 11.3 km/h (7 mph), a test of three seconds for TCP, three seconds for UDP, and three seconds to collect GPS information allowed one complete round of tests to be completed every 28 m (92'), as shown in Figure 4.5. This procedure was automated using a custom Python 2.7 script, which ran the TCP test, collected GPS information, ran the UDP test, and repeated the process continuously. The code for this testing can be found in the online repository at https://github.com/thiemep/TPAC-Wifi . Figure 4.4 shows the raw output from one round of network connection testing, while Table 4.1 shows the associated labeled output from iperf for both the TCP and UDP tests.
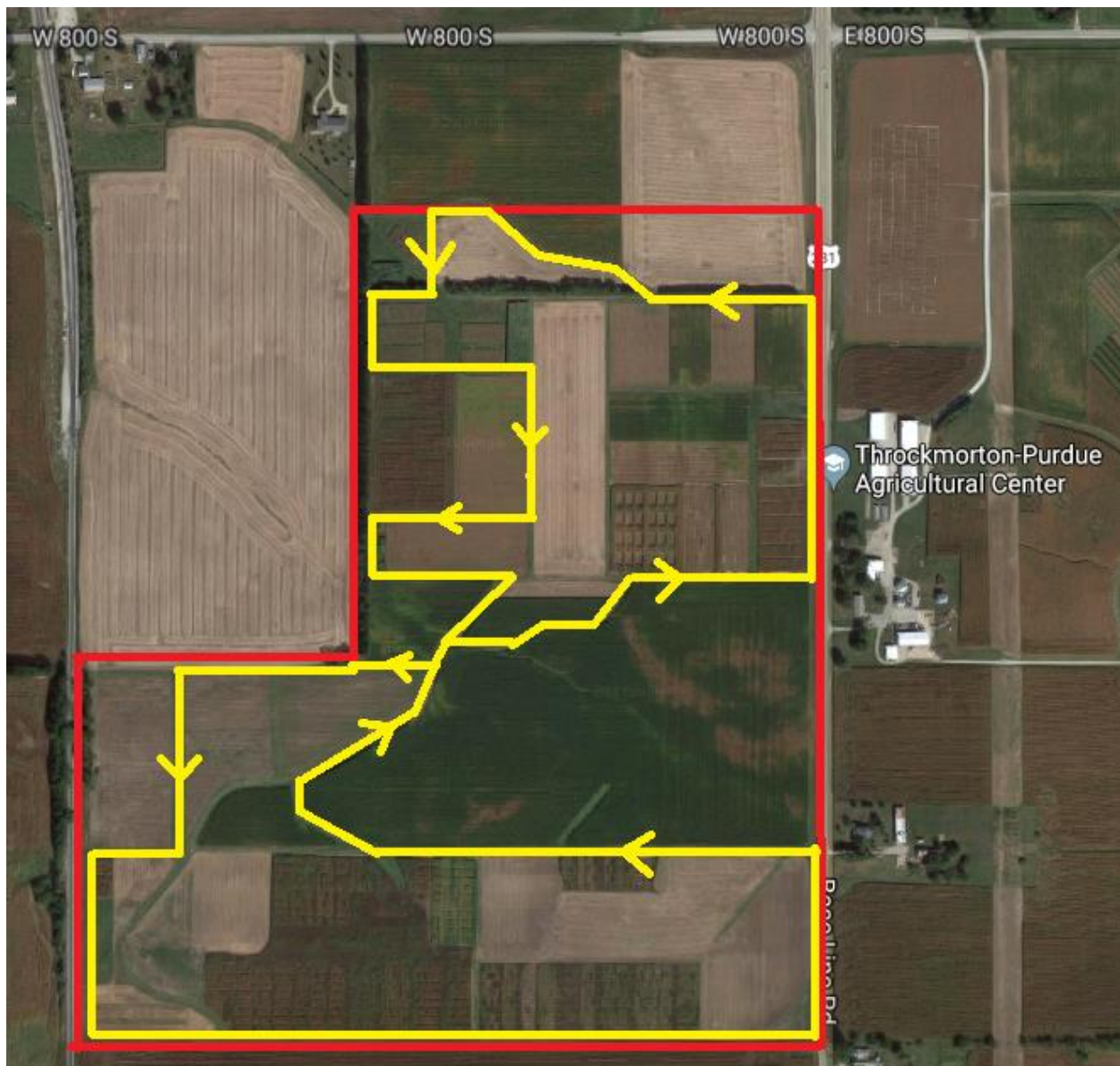
Figure 4.3: Route of the Tractor Client

1 2019-10-23T19:31:24.000Z

TCP TEST: 4.82 1645

[225.73575, 40.29301101525, -86.90382730525]

UDP TEST: 0.00-3.00 376 125 5.519 0/47 (0%)

Figure 4.4: Raw Output of Network Connection Test

Table 4.1: Labelled Output of Network Connection Test

Antenna No.	Date and Time	Test Type	Transferred (MB)	Bandwidth (KB/s)
1	2019-10-23T19:31:24.000Z	TCP TEST:	4.82	1645

Altitude (m)	Latitude	Longitude
225.73575	40.29301101525	-86.90382730525

Test Type	Time Duration	Transferred (KB)	Speed (KB/s)	Latency (ms)	Dropped Packets	Percent Loss
UDP TEST:	0.00-3.00	376	125	5.519	0/47	(0%)
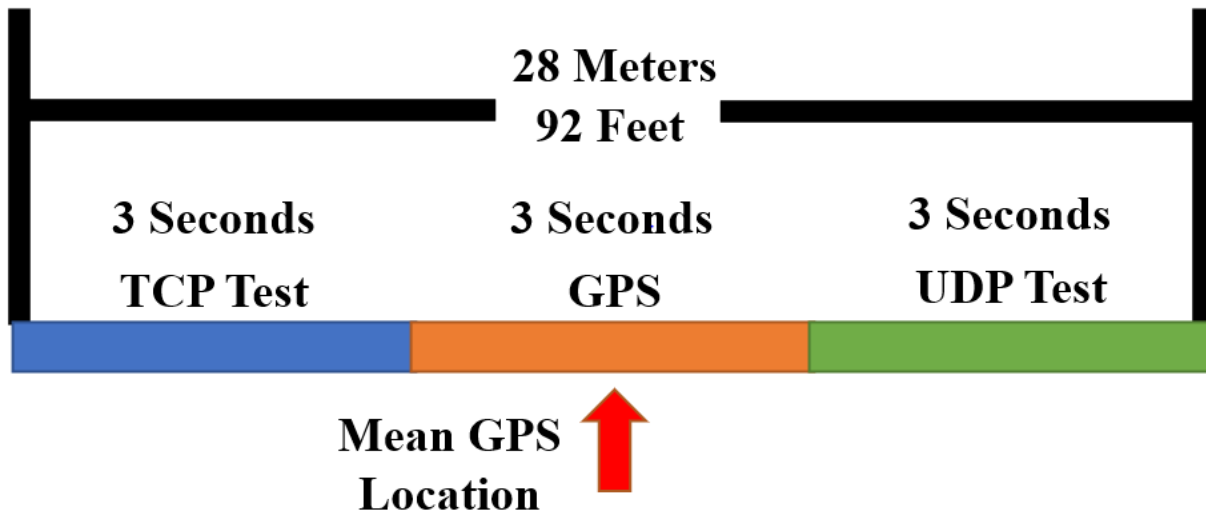
Figure 4.5: Visual Representation of One Test Cycle

With each run of the network test script, the GPS location was recorded. GPS data was collected using a USB GPS receiver which utilized the U-Blox 7 chipset (U-Blox, Inc., 2018). The U-Blox 7 chipset had the capability to use the wide area augmentation system (WAAS), which used additional satellites to increase the accuracy of GPS readings. With WAAS enabled, an extended test of GPS measurement in addition to the stationary test described in Section 3 was performed. The stationary test showed that its standard deviation was at most 1.38m (4.5'). After initial setup, a test route was driven with the GPS to test its ability to track the tractor when driven along a predetermined course. The resultant GPS path can be seen in Figure 4.6, which

51

was generated using the website www.gpsvisualizer.com. After these tests it was determined that the GPS was reliably accurate enough to trust its readings to within the tractor's wheel base of 3m (10').

Figure 4.6: Initial GPS Test Track

During operation when network measurements were being taken, the GPS collection portion of the testing cycle was placed in between the TCP and UDP measurements. This was to ensure that the location the GPS recorded would be equally representative of the location at which the TCP test was performed and the location at which the UDP test was performed.

To study the effect of gain on connection properties, two antennae were used on the client machine. A high gain antenna of 18dBi and a low gain antenna of 8dBi were both used in the same manner as described above. At the conclusion of each testing sequence, an RF switch was flipped, connecting the transceiver to the opposite antenna as logged in Table 4.1. Because of this alternation between high and low gain antennae, the route was driven twice on each data collection day. This was done to increase the number of points where data was collected, as well as to provide multiple measurements throughout the route to either reinforce existing measurements which were similar, or discredit measurements that were outliers.

Full sets of measurements were taken three times weekly, on Monday, Wednesday, and Friday, as close to solar noon as possible, to decrease any variation in signal properties that could result from the time of day. Due to the incredibly wet spring, agricultural equipment was unable to enter fields at the standard time of the season due to high risk of rutting or becoming stuck. Therefore testing began in early June, before crops had emerged and after the wet ground had

dried. Testing was continued throughout the growing season until early November, when the majority of crops had been harvested.

4.3 Stationary Data Collection

In addition to the tractor which collected data as a mobile client, there were three stationary sensors that also measured network properties. These sensors were meant to simulate the type of hardware that would be used for weather stations, soil sensors, remote cameras, or other stationary devices that might need to send information wirelessly. Since the task was very similar to that of the tractor, many of the same components were used in-system to connect to the network. The system used to collect stationary network connection information was discussed in Section 3.

As can be seen in Figure 4.7, three such sensors were placed in the field to record network properties. Their mode of operation was nearly identical to that of the tractor. Iperf was used as the connection measurement program, which was run with custom python scripts to facilitate the measurement of network characteristics. The sensors also employed nearly all of the same hardware components as were found in the tractor. Differences between the two systems included a different loadout of antennae, supporting RF switchgear, and power supply
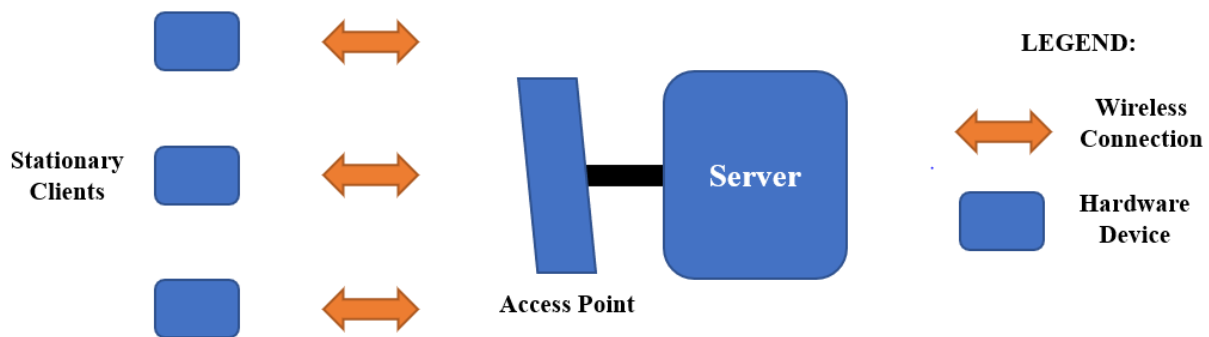
Figure 4.7: Stationary Client System for Network Properties Measurement

components. Since the sensors were to be stationary and maximizing the efficiency of bringing power to the units was not the goal of the project, 12V deep cycle marine batteries were used to power all components. Since the Ubiquiti Bullet was powered over PoE, which was a Ubiquiti standard at 24V, a step-up transformer was necessary. While two 12V batteries in series could

have been used for the PoE, the Udoo ran on 12V and would not accept a 24V input, and would require regulation down to 12V if two batteries were used in series.

Another difference in hardware between the mobile and stationary clients was the lack of a high gain antenna on the stationary sensors. Each sensor was mounted by driving a 2.1 m (7') t-post into the ground, until the winglets of the t-post were beneath the surface of the soil. This resulted in a 2 m (6') post for mounting sensors. This method was chosen, because it was easily removable, easy to install, a common method of mounting objects in a field, and used resources readily available to farmers all over the country. As a result, the steel t-post provided an excellent support on which to mount electronics. Electronic components were housed inside a waterproof enclosure and fastened to the post. Because the post was ferric and driven into the ground, only one antenna was used to make network measurements for fear of electromagnetic coupling with the t-post. A second antenna, provided the first was mounted at the top of the post, would need to be mounted elsewhere on the post, below the first. This would create different spatial environments for the two antennae, making a comparison of characteristics due to gain or height differences between the two useless.

Locations of the sensors were chosen to best measure network properties at varying distances from the access point. As such, the greatest radial distance available from the access point was used. This was the line connecting the access point and the south-westernmost corner of the area of interest, as shown in Figure 4.8. A distance of 1,182 m (3900 ft) was the largest distance usable on the property from the centrally located access point. Since the antennae were placed only 2m (6') in the air, corn would eventually reach a sufficient height to block the line of sight between the antenna of the sensor and the access point. This effect was to be measured, so the sensors were placed at the immediate edge of field sections towards the access point. To prevent damage from sprayers or combines in the field, each sensor was placed along the edge of a grass path, and an orange flag attached to the top for added visibility. Figure 4.9 shows sensor number one, the closest sensor to the access point, post-harvest.
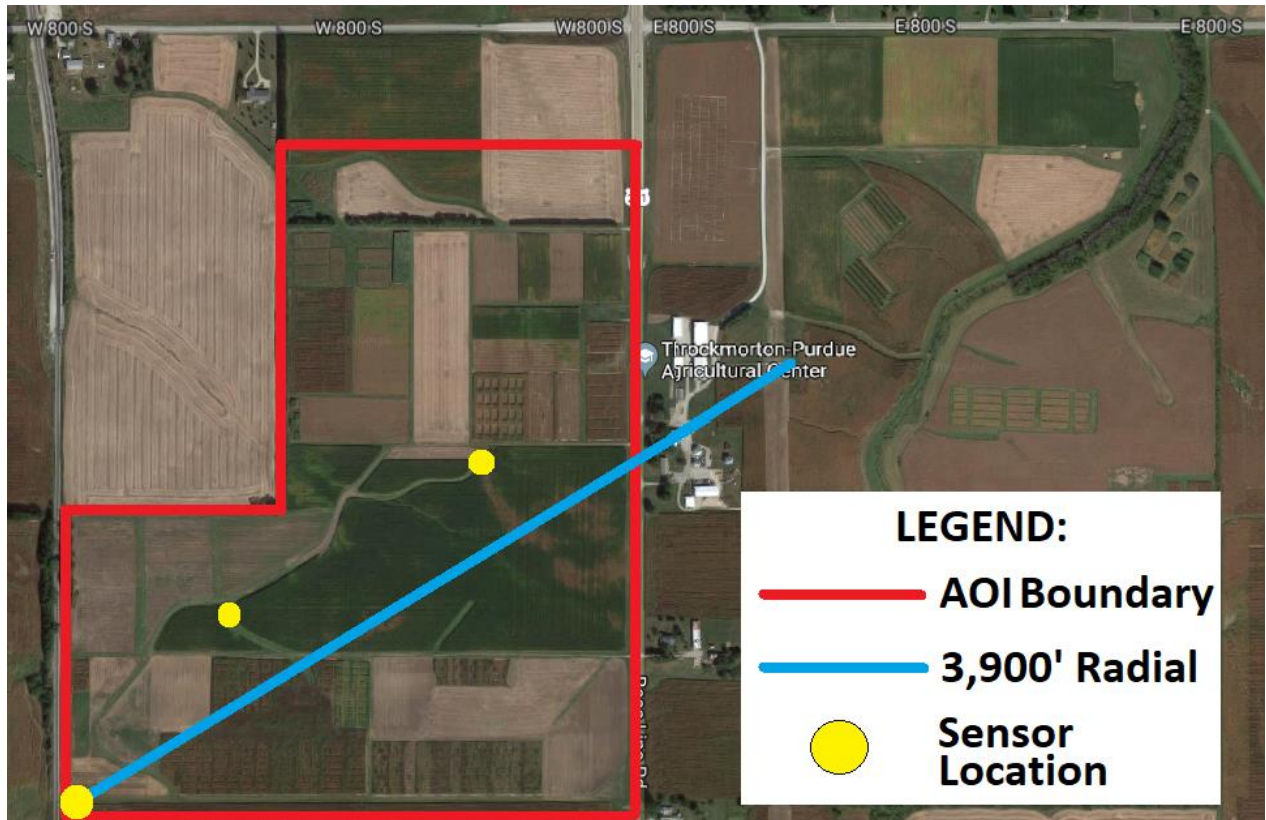
Figure 4.8: Stationary Sensor Locations

GPS location of each sensor was recorded using Google Maps and referenced during data analysis. The coordinates of each sensor, along with the access point, can be found in Table 4.2. While the tractor data collection system was programmed so that the user had to initiate a testing event, the field sensors began their tests automatically. Measurements were taken hourly, with sensor one, the closest to the access point, performing its measurements first. Every six minutes thereafter, another sensor would run its tests, until all three had finished for the hour. Tests were staggered in this way due to the inability of the server at the access point to process simultaneous connection requests. Each sensor collected six measurements inside each test window at the top of the hour, which took a total time of 36 s. Since there was no GPS location poll, the total measurement event took only 6 s, as opposed to the tractor's 9 s. Since the server could not support multiple simultaneous connections, time was left in between sensor measurements to allow the tractor to connect if it was also taking measurements around the top of each hour.

Figure 4.9: Field Sensor # 1 After Harvest

Table 4.2: GPS Coordinates of Stationary Sensors and the Access Point

Location	Latitude	Longitude
Access Point	40.297114	-86.901049
Sensor Number One	40.295948	-86.906231
Sensor Number Two	40.293982	-86.910362
Sensor Number Three	40.291688	-86.913127

4.4 Environmental Considerations

The environment was anticipated to be the single most important variable in the entire project. Over the duration of the project there were occasional rainstorms, along with normal temperature and precipitation variation. Certain environmental conditions were monitored and recorded for later analysis alongside the network information previously discussed. The recorded environmental conditions were determined to be those that could have the greatest impact on network characteristics. Specifically, these environmental characteristics of interest are the height of crops, changes in the terrain, blockage of the signals by obstacles such as trees or crops, precipitation, soil moisture, and the time of day at which measurements were taken.

Because TPAC is a research farm for the College of Agriculture, plots of land are often subdivided into smaller plots for research purposes. This led to moderate levels of heterogeneity in the crop cover, as may not typically be the case on a large-scale production crop farm. The area of interest seen in Figure 4.8 had the largest contiguous field on the farm in its southern half. This was another reason that the particular area of interest was chosen. Because of the diversified crop species, the height of crops throughout the season were measured in multiple places. Ideally, the height of every research plot would have been measured, but due to time constraints this was not a realistic or feasible goal. Instead, crop heights were measured in the three largest plots. Figure 4.10 shows the locations of crop measurements, in addition to the species of crop planted in various locations around the area of interest.
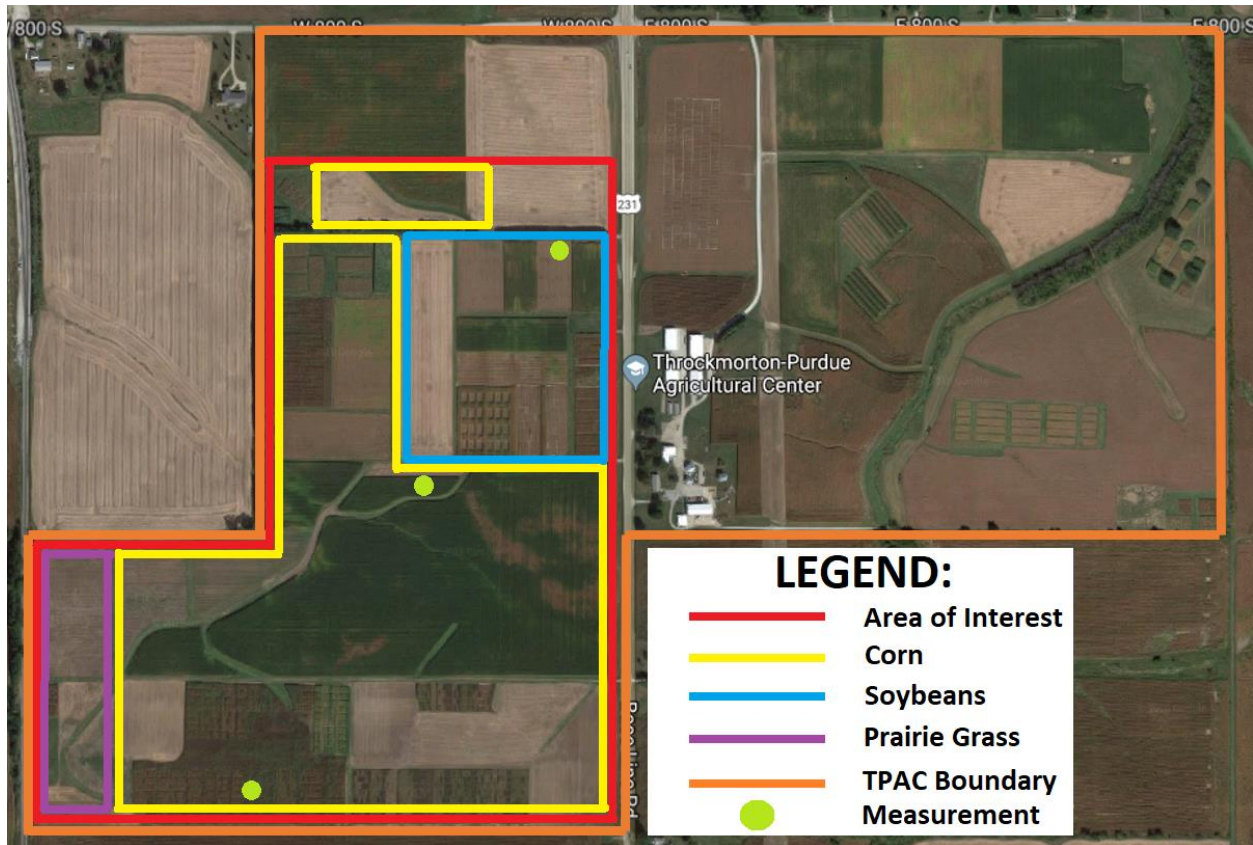
Figure 4.10: Crop Types Planted Throughout the AOI

Purdue is located in central Indiana, where the terrain is relatively flat. Variations in landscape typically are limited to valleys and hills of rarely more than 15m (50'). TPAC is no exception from this rule, as the entire property has no major valleys or hills. For the purposes of this experiment this would make it difficult to measure a difference in wireless connection properties based solely on elevation change. Within the area of interest, there was one depression spanning the length of the property for drainage purposes, but this depression was less than 1.5m (5') in depth, making the area of interest essentially very flat. Similarly, trees were not expected to play a large role either, as the TPAC landscape was largely devoid of trees. The most notable locations where trees interfered with line-of-sight to the access point were at the border between the northernmost cornfield and the field of soybeans.

Precipitation records were obtained from a weather station hosted at TPAC, whose information was made public through the National Oceanic and Atmospheric Administration (NOAA) (United States National Oceanic and Atmospheric Administration, 2019). This data was used to record the time of precipitation events, their duration, and their potential effect on

network connection properties at long range. Information gathered from the weather station at TPAC was incomplete. Thus when applicable, supplementary weather information was sourced from the weather station at the Purdue University Airport (KLAF). Two precipitation derivatives were computed to ascertain the effect of moisture in the air, higher soil moisture, and surface moisture on the plants: a three-day running total (sum) of precipitation, and the sum of the previous two days' worth of rainfall.

4.5 Data Analysis

At the close of the growing season, after all crops had been harvested and all hardware removed from the field, the four Udoo x86 computers were accessed and the files they had generated were copied. Each computer made a separate file for each day, and these files were sorted by machine and time. The first step in the analysis process was data cleaning. Since the data was stored as plain, space-delimited text files, they were imported into Microsoft Excel and saved as comma separated value (CSV) files for later manipulation. After this had been completed for all data, reordering was performed next.

Data reordering consisted first of removing unwanted inputs. For example, as shown in Table 4.1, the value "TCP TEST:" was recorded with each data collection cycle. While useful for the human observer, this string provides no useful information for the computer used to sort and analyze the data, so it was eliminated from all the files. Similarly, the "UDP TEST:" marker was removed as well. The data was then scrubbed of all non-numerical characters like commas, brackets, and punctuation excluding decimals. Since the data was already in Excel for this procedure, Visual Basic was used to write a program to perform this data cleaning. The program can be found in the online repository at https://github.com/thiemep/TPAC-Wifi .

4.5.1 Georeferencing of Tractor Data with MATLAB

Once cleaned of superfluous entries, the cleaned CSV files from the tractor were imported into MATLAB. While Excel has matrix processing capabilities, MATLAB has native support for georeferencing data. Once imported, each day's data was parsed for the GPS coordinates of each reading and sorted accordingly. One problem with the method described for the client machine was the relative sparseness of points collected. Even driving the route shown in Figure 4.3 twice, only 120-140 measurements were taken, depending on the tractor speed, for the whole area of interest every two passes. Not only was this not enough data to create a usable heatmap of the area, but the data points were arranged in an irregular fashion. Because of this, a polar coordinate system was used to divide the data into polar sectors – the contents of which could be averaged to better allow graphs, charts, and tables to be generated. This was done for tractor data only.

To accomplish this, the area of interest was divided as shown in Figure 4.11. A sample of the route driven is included in the figure to help give a sense of scale to the image. By dividing up the area of interest into polar sections, each sector can be defined as having a certain distance from the access point, allowing direct comparisons to be drawn between sectors based on range. Similarly, by providing angular boundaries to sectors, any variation due to the beamwidth of the access point could be identified. Once the MATLAB script had finished, each data point was assigned a label, with label identifiers from A1 to J8, depending on distance and angle from the access point, as shown in Figure 4.11. However in practice, only the sections through which the tractor path passed were assigned data. This allowed future sorting and averaging of data within each sector to proceed with greater ease.
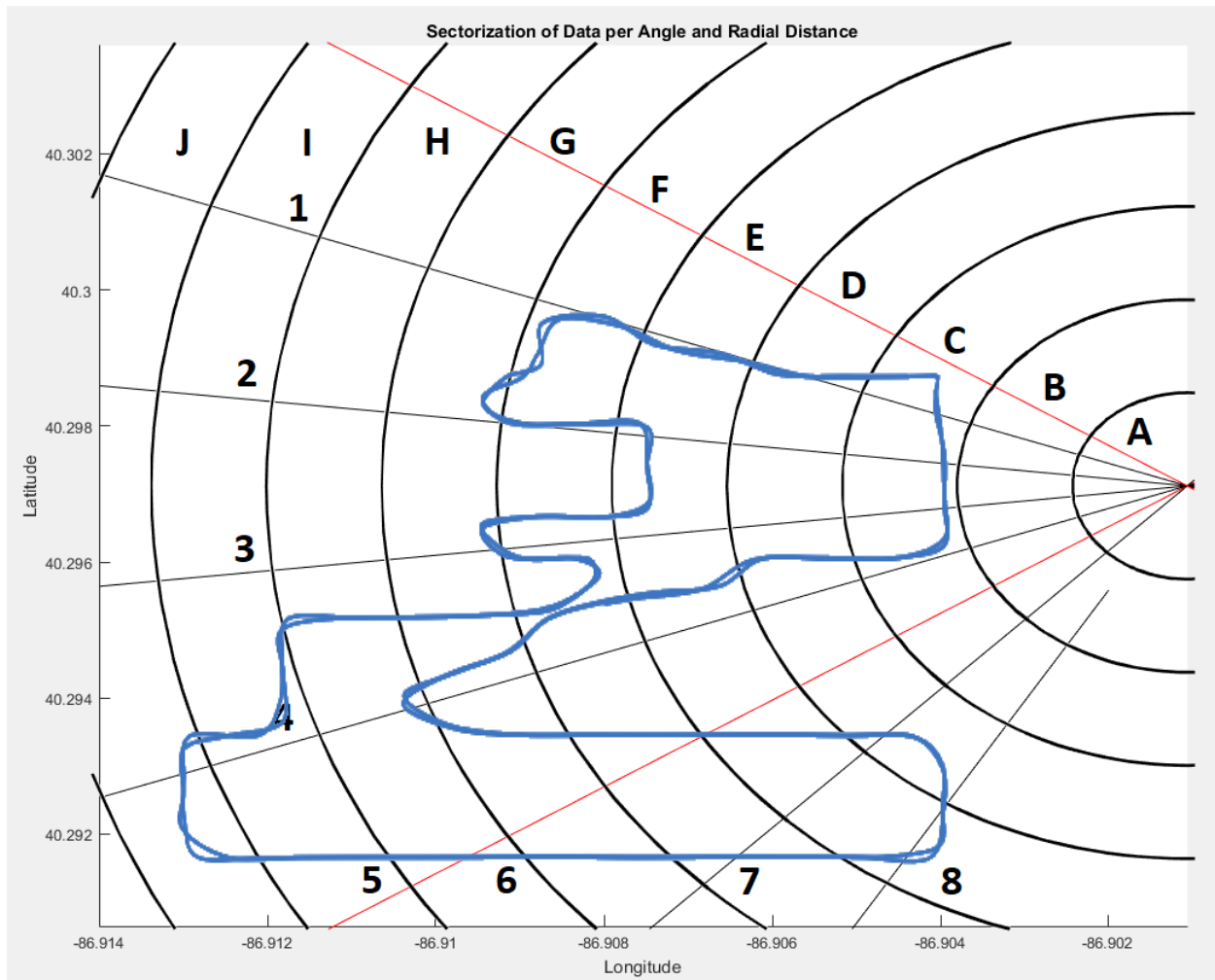
**Figure 4.11: Polar Division of the AOI, With Actual Tractor Path
in Blue and Access Point Coverage Boundaries in Red**

The final step of geospatial data processing before signal analysis could be performed was
the averaging of data points relative to their location. As mentioned previously, all data points
within each sector shown in Figure 4.11 were blocked into 80 distinct data points. For this
purpose, each day's worth of data was entered as a separate sheet in Excel. A "summary sheet"
was then created that referenced the data on each sheet, which were all formatted in exactly the
same way. This cross-linking is illustrated in Figure 4.12.

61

Summary Sheet Throughput

Day	A1	A2	A3	A4	...
1	1234	1342	1324	1243	...
2	2342	2342	2324	2243	...
...	...	...	...	...	...
N	3234	3342	3324	3243	...

Summary Sheet Latency

Day	A1	A2	A3	A4	...
1	10	12	14	16	...
2	20	22	24	26	...
...	...	...	...	...	...
N	30	32	34	36	...

Day 1

LOC	THROUGHPUT	LATENCY	...
A1	1234	10	...
A2	1342	12	...
A3	1324	14	...
A4	1243	16	...
...	...	...	...

Day 2

LOC	THROUGHPUT	LATENCY	...
A1	2234	20	...
A2	2342	22	...
A3	2324	24	...
A4	2243	26	...
...	...	...	...

Day N

LOC	THROUGHPUT	LATENCY	...
A1	3234	30	...
A2	3342	32	...
A3	3324	34	...
A4	3243	36	...
...	...	...	...

Figure 4.12: Relationship of Summary Sheets to Sorted Data

4.5.2 Statistical Regression Analysis in Excel

Collected data was imported into Excel and models for potential predictors (Table 4.3) were developed using regression. The process was identical for mobile data as with stationary data, except the stationary sensors had no GPS data.

Regression analyses were performed to determine if any relationships existed between the network characteristics and potential predictors shown in Table 4.3. Linear regressions were performed on each independent variable to each network characteristic: throughput, latency, and the number of dropped packets. A confidence value of 95% was set ($\alpha = 0.05$) as a threshold to judge significance. Thus, each regression coefficient needed to have a p-value less than or equal to 0.05 to be considered significant.

Table 4.3: List of Dependent and Independent Variables

Independent Variables (Potential Predictors)	Dependent Variables (Network Properties)
[ANG] Angle to Access Point (Tractor Only)	[TPT] Throughput
[DIST] Distance from Access Point	[LAT] Latency
[3DPRCP] 3-Day Precipitation Total	[DROP] Dropped Packets
[2DPRCP] Prior 2-Day Precipitation	
[YESTR] Prior-Day Precipitation	
[CORN1, CORN2, SOY] Crop height	
[MEANTEMP] Daily Average Temperature	
[ANT] Antenna Gain (Tractor Only)	

A multivariate linear regression was performed including all potential independent variables for each network characteristic to determine whether an individual predictor remained significant in the presence of other predictors in the model. As before, predictors with p-values of less than 0.05 in the multivariate model were recorded for each network characteristic. From these analyses, only predictors with 95% statistical significance were used in the creation of a prediction model for each network characteristic. This resulted in one model for throughput, one for latency, and one for dropped packet count. R-values were noted to determine how well each model fit the data.

4.6 Assumptions

During the execution of this project, there were inevitably assumptions about many variables in the system that had to be made. Many of these assumptions could be independently studied or calculated, but these efforts could be exceedingly time consuming and, in many cases, would stand as research projects in their own right.
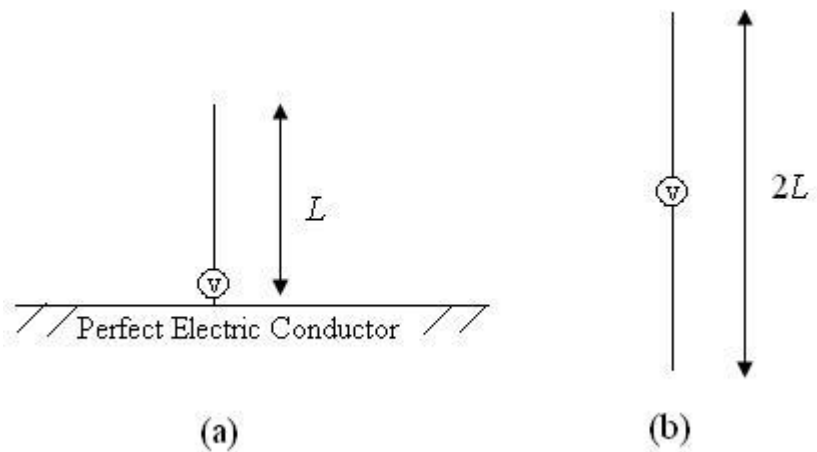
Figure 4.13: A Monopole Antenna (a) and a Dipole Antenna (b) (Bevelacqua, 2011)

The first assumption was made with regards to the cab of the tractor. Since the tractor had two antennae mounted above its roof, and they were firmly grounded to the frame of the vehicle, it was assumed that the metallic roof of the tractor provided a sufficient ground plane to support both antennae. For any vertical radiating monopole antenna, it is important to have an orthogonal plane beneath that is electrically conductive and tied to ground. This is the case, because of the nature of a monopole antenna. It induces a wave in the air without having a second monopole of opposite polarity as is the case with the dipole antenna. A schematic of a monopole antenna and dipole antenna can be seen in Figure 4.13. By inserting a conductive ground plane at the base of the monopole, a reflection of the antenna appears in the ground as a second monopole of opposite polarity. This phenomenon is called the Image Theorem (Chew, 1990).

Similarly, it was assumed that the antennae on the cab would not interfere with each other's radiation patterns. Since the RF switch used was of the SPDT type, each antenna was not connected to ground when it was not in use. The antenna was left to 'float', since it was neither being driven by the transceiver nor was it grounded to the frame of the vehicle. Had the antennae been connected to ground when not in use, they would have coupled with one another, as they were in the near-field region. The near-field region of an antenna is the distance inside of which the electric and magnetic fields are out of phase with each other by ninety degrees, as opposed to the far-field where radiated waves are in phase. More commonly, this area around an antenna can

be identified by a change in signal properties when an object is brought near. For example, when using a car stereo to receive a weak broadcast station, bringing your hand near to the antenna causes the signal strength to change. This is because objects within the near field region alter the tuning of the antenna and cause an impedance mismatch. The near field distance is defined by Equation 4.1:

Eq. 4.1 $$R < 0.62 \sqrt{\frac{D^3}{\lambda}}$$

Where: R = Near Field Boundary (m)

D = Antenna Major Dimension (m)

λ = Wavelength (m)

For the larger of the two antennae, the Hawking 15dBi high-gain antenna operating at a frequency of 2.4Ghz, this distance was 2.36 meters, which was wider than the tractor cab. When installing components of ground-based systems, it was assumed that proper ground contact with the Earth was being made. For reasons described previously, the importance of a proper ground connection in RF systems was imperative. While the access point antenna was properly grounded by connecting the coaxial cable to the tower's frame, the field sensors were only mounted on steel posts driven a foot into the ground. This was perhaps the weakest ground point in the entire project, and it was assumed that the contact was "good enough" to not affect the propagation characteristics.

It was assumed that by mounting the access point on the broadcast tower for WBAA, that the site would present similar environmental characteristics to a similar zone located atop a grain elevator, as is much more common on production farms. Inherent in this assumption was the idea that for an access point mounted on a grain elevator, it would be located well above any nearby grain bins, as such bins would cause RF shadowing in the direction of the bin.

Inside the tractor cab, all components in use were assumed to be lossless and non-radiative after initial testing and setup. This included all of the coaxial cable, which was assumed to be lossless and a perfect conductor of RF energy. Similarly, the RF switch used to alternate between roof-mounted antennae was assumed to be a perfect match of 50+0j, since the standing wave

ratio (SWR) and return loss measurements were within acceptable limits. The switch was also assumed to be a perfect isolator between the transceiver and the deselected antenna.

Finally, it was assumed that the program iperf3 would utilize the full extent of its network connection ability. If this were not to be the case, then the test would not be a true measurement of the limits available to such a system regarding network properties. It was implied in this assumption that the wireless link propagation characteristics themselves would be the bottleneck in the system, and not any component, interface, or protocol. These results were previously discussed in Section 3 and are expanded upon in greater detail in Section 5.

4.7 Mid-Season Data Loss Event

All of the data collected mid-season was lost due to damage caused by a lightning strike. While the server could still be contacted to establish a connection between it and the sensors, the speed of the system was limited. The details of this event must be covered before results of the experiment can be discussed.

On either day 28 or 29, (June 30th or July 1st), a fault in the system manifested itself by speed limiting all connections to the server to almost exactly 10Mb/s. Recognizing there was a fault, a diagnostic of every system component was performed starting with the mobile sensor system. When no faults were found in the mobile system, the access point was inspected for damage. After nearly three weeks of troubleshooting, the problem was narrowed to the Ubiquiti Bullet M2 used as the access point transceiver on the tower. The Bullet was initially checked for errors, but passed over because it still provided wireless and wired communication between the router and wireless clients. It was only upon further investigation that the ethernet rate controller was found to be damaged, and reverting to its lowest negotiable connection speed of 10 Mb/s.

Once a tower climber could be hired, the transceiver was replaced and the system returned to normal operation. This unfortunate event resulted in the loss of six weeks of mid-season data, and the results discussed in Section 5 are based on data collected at either end of the season. Figures showing collected data have been made without this erroneous data.

5. RESULTS

5.1 Brief Overview of Analysis Techniques

Data collection and processing techniques were covered in section 4, but a brief review will be provided for context, before the data results are presented. As shown in Figure 4.4, data was saved to file using the program iperf3 to capture network properties. This file was then parsed using Microsoft Excel, the product of which is shown in Table 4.1. All data was then manually searched for artifacts like empty cells, improper data type, or improper formatting to facilitate automatic manipulation in the processes to follow. For data from the tractor, the cleaned data was imported to MATLAB and sorted into polar sectors about the access point, as shown in Figure 4.11. The sorted data was then exported back to Excel for analysis alongside the rest of the collected data.

For the first part of the analysis, to facilitate the generation of graphical tables and to allow a better characterization of the physical space, the georeferenced tractor data imported from MATLAB was sorted by location first using radial distance and second by angular position. Following this sort, each data point in a given sector was averaged with the other data points in that sector. By ordering these two sets of transformed data by hour and position respectively and by placing all tabs of the same data type in an Excel worksheet, it was possible to reference every collected data sheet using a summary page, as each data sheet was formatted identically. Data could be parsed from amongst the separate tabs in Excel as needed to perform comparisons, ask statistical questions, and create graphics.

The second part of the data analysis was performed using Excel's built-in data analysis tool pack. Tractor data was concatenated into one spreadsheet, and sensor data was sorted into one spreadsheet. Every potential predictor and every measured network characteristic was present in each spreadsheet. Single and multiple linear regressions were then performed on the data to determine if any statistically significant relationships existed between the data types shown in Table 4.3. From these, the best predictors were used to make linear models that attempted to explain the measured characteristics. Throughout this analysis, the five objectives for the project specified in the introduction were addressed.

5.2 Data Overview

Before statistical analysis, one final round of data cleaning needed to be performed. A failure of a component in the system led to instability in all collected data, before the problem was fixed. This data was removed, as it was neither reliable nor representative of actual wireless propagation characteristics at the time. The problem was presumably due to a lightning strike on the WBAA broadcast tower. Despite the efforts that were made to prevent any sort of discharge from damaging the system, the Ubiquiti Bullet which ran the access point was damaged around July 1st, 2019. This will be discussed further in Section 6, but it should be noted that this event rendered all data between July 1st and August 19th useless.

In addition to the data collected by the experiment, weather information was obtained from a repository of historical weather conditions recorded by a weather station at TPAC. This was done through NOAA's website (United States National Oceanic and Atmospheric Administration, 2019), where a CSV of precipitation and maximum and minimum temperatures was obtained for the time period of the experiment. This data was first plotted singularly, as can be seen by the records of temperature and precipitation shown in Figures 5.1 and 5.2, respectively. It is important to note that the NOAA TPAC weather site did not provide a reading for each day. A significant minority of the days in the time of interest were without data. This was supplemented with weather information from the Purdue airport, KLAF.

The average daily temperature was not given in the weather station reports from TPAC or KLAF, so the average daily temperature was assumed to be two thirds of the value between the absolute maximum and minimum temperatures recorded that day. This computed average daily temperature can be seen in Figure 5.1. The rainfall events shown in Figure 5.2 were used to estimate the effect of precipitation on the environment by adding days of precipitation together. This was accomplished by adding the amount of rainfall for the preceding three days for each day and adding the rainfall for the prior two days to each measurement. These measurements were chosen because soil moisture data was not available and they also serve as a proxy for surface moisture on plants. The equations were Equation 5.1 and Equation 5.2, respectively. The computation used for average temperature is shown in Equation 5.3.
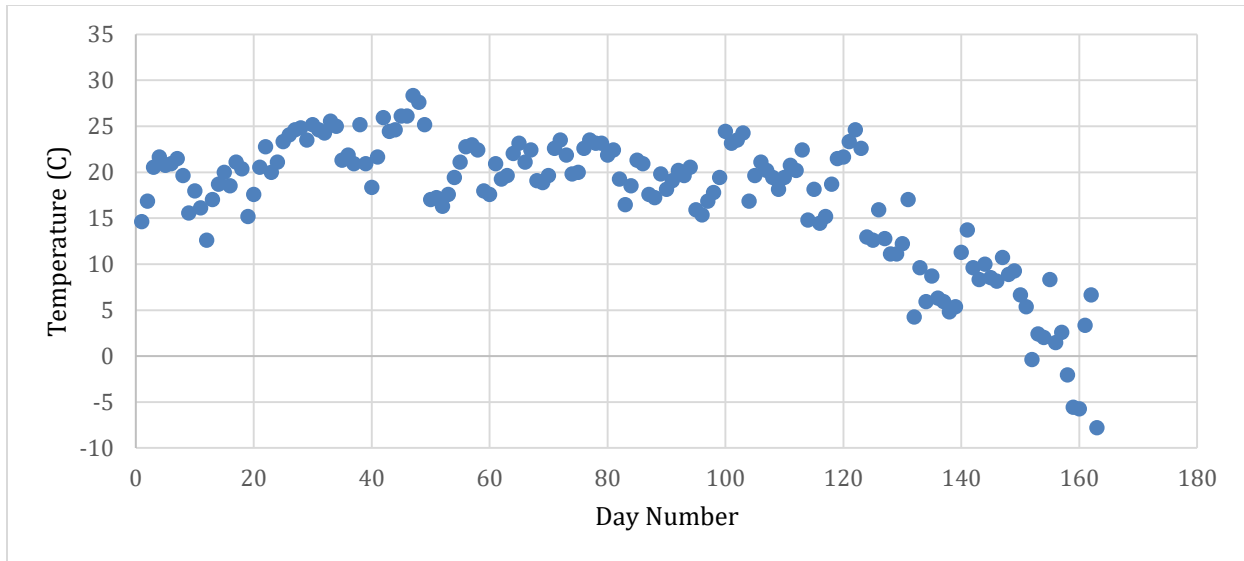
**Figure 5.1: Computed Average Temperature
Measurements over the Time of Interest at TPAC**
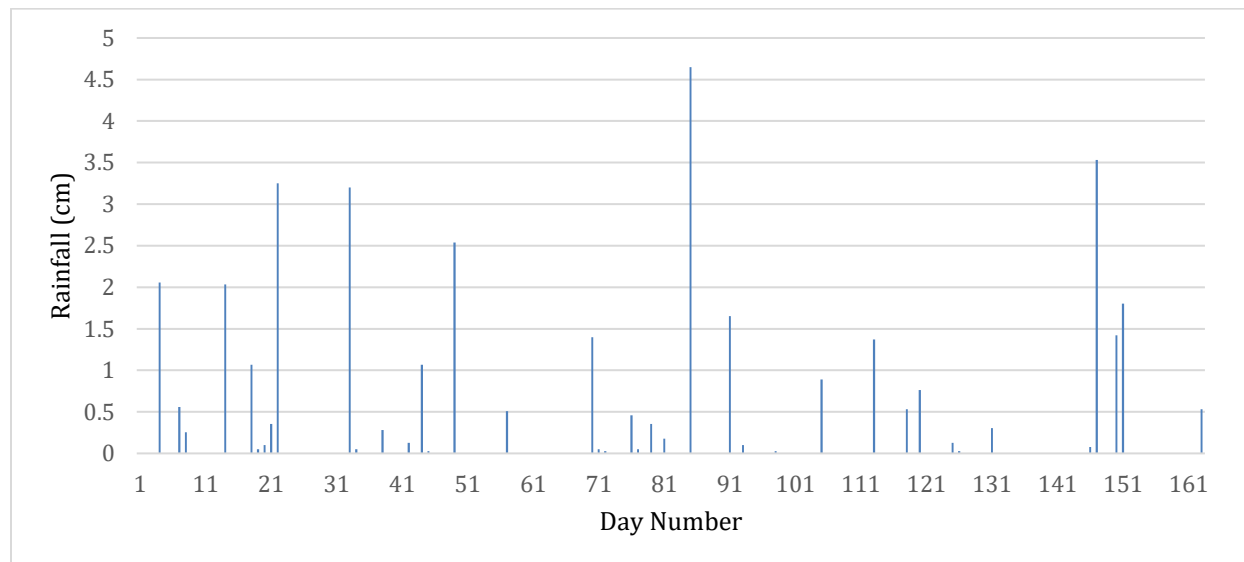
Figure 5.2: Rainfall Events over the Time of Interest at TPAC

Eq. 5.1
$$P_{3D} = \sum_{i=-2}^{0} P_i$$

Where: P_{3D} is the three day running total

i is the day signifier, with $i = 0$ being the current day

P_i is the precipitation for day i.

Eq. 5.2
$$P_{2D} = \sum_{i=-2}^{-1} P_i$$

Where: P_{2D} is the sum of rainfall for the two preceding days

Eq. 5.3
$$T_{AV} = T_{MAX} - \frac{1}{3} * (T_{MAX} - T_{MIN})$$

Where: T_{AV} = Average Daily Temperature

T_{MAX} = Maximum Daily Temperature

T_{MIN} = Minimum Daily Temperature

For each day, the composite precipitation would be dependent on the precipitation of the days leading up to the day on which the measurements were being taken, so both of these methods were used to attempt to describe how much water was present in the environment. These composite measures can be seen in Figure 5.3 and Figure 5.4.
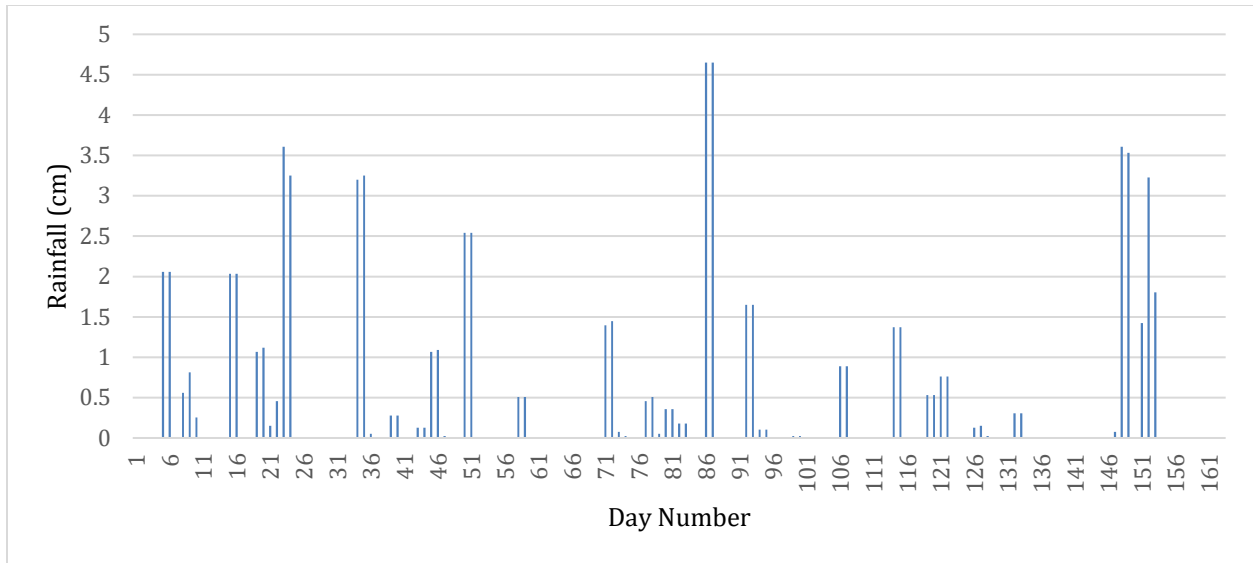
Figure 5.3: Record of Summary Rainfall for Prior Two Days for Every Day
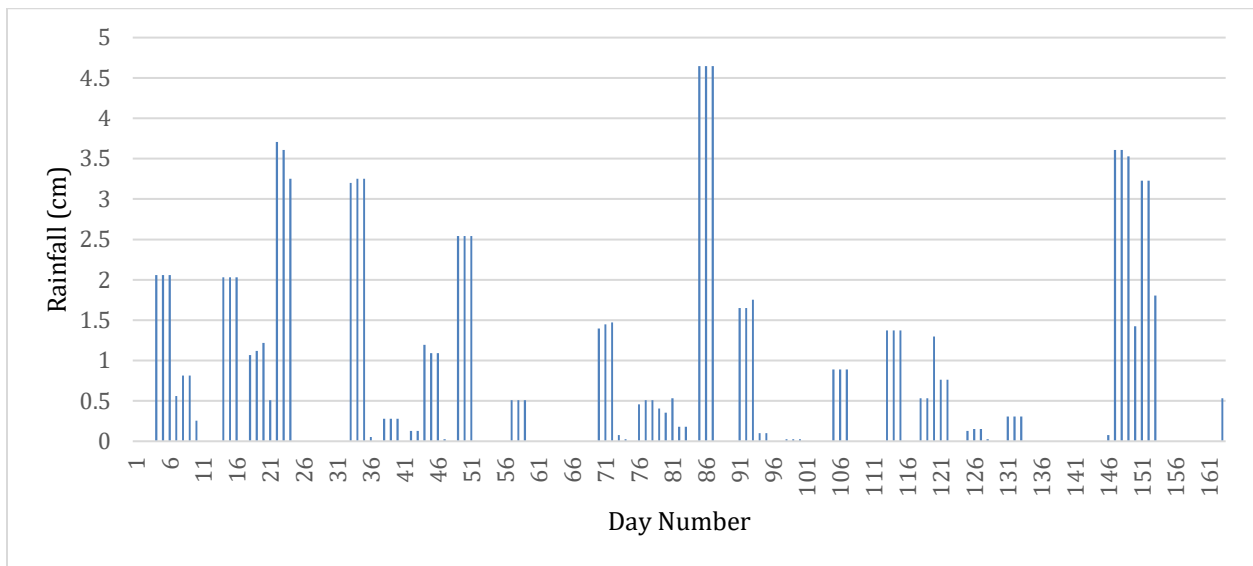
Figure 5.4: Three Day Running Total of Rainfall for Every Day

Once weather data had been entered into the spreadsheet and viewed, crop height data was manually entered from a notebook into the sheet and graphed. Figure 5.5 shows crop heights at the three locations shown in Figure 4.10, where "Corn 1" represents the southernmost measurement location, "Corn 2" provides the center measurement location, and "Soybeans" illustrates the northernmost measurement location. It should be noted that once the crops reached

71

full height, as confirmed by two weeks of measurement without change, height measurements were ceased, and the final height was assumed for the remainder of the growing season.
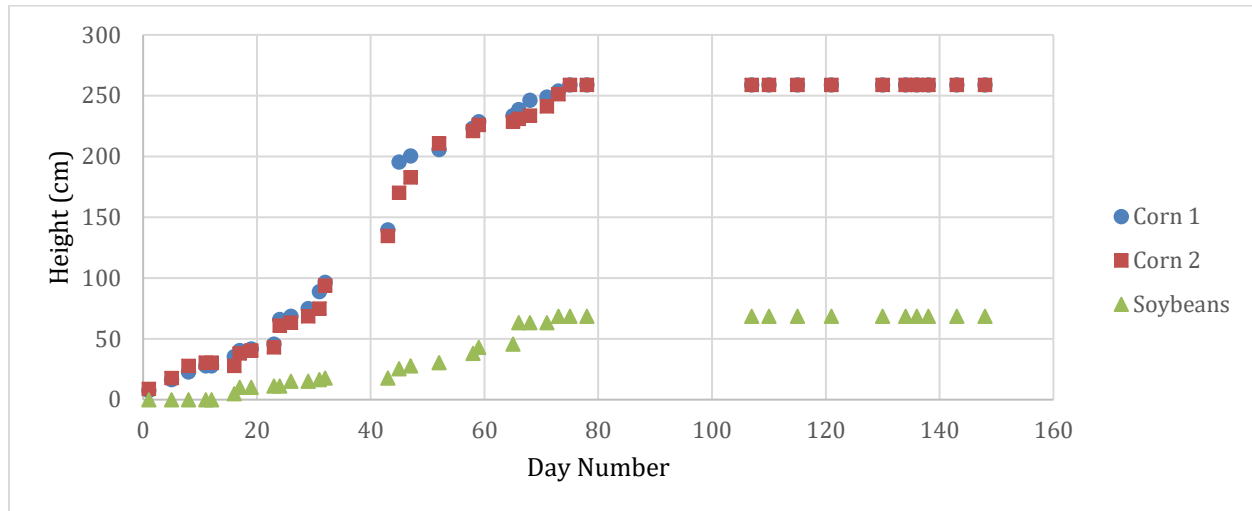
Figure 5.5: Crop Heights Over the Time of Interest

5.3 Positional Analysis via MATLAB and Excel

With environmental considerations entered into the workbook, visual representations of the data collected regarding network characteristics were created. In raw form, these were graphs of network characteristics over time and space. Figure 5.6 shows a sample of this data as throughput capacity on the high-gain tractor antenna along the radial "4" for all distances. Similarly, Figure 5.7 shows the same data for the low-gain antenna. Figure 5.8 shows the same throughput data along a line of constant radius "F". Similarly, low-gain data is shown in Figure 5.9 for the constant radius "F". To observe these locations, refer to Figure 4.11. As mentioned previously, data between July 1st and August 19th is omitted for data purity purposes.
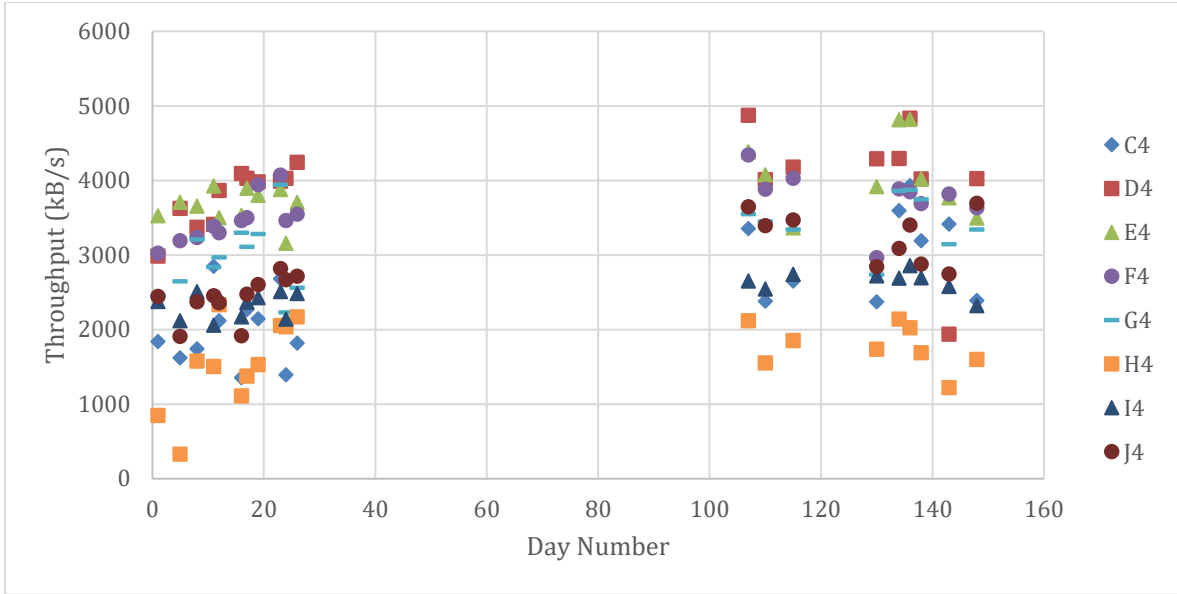
**Figure 5.6: Sample of High-Gain Antenna Throughput vs. Date
for Selected Sectors Along a Line of Constant Angle**
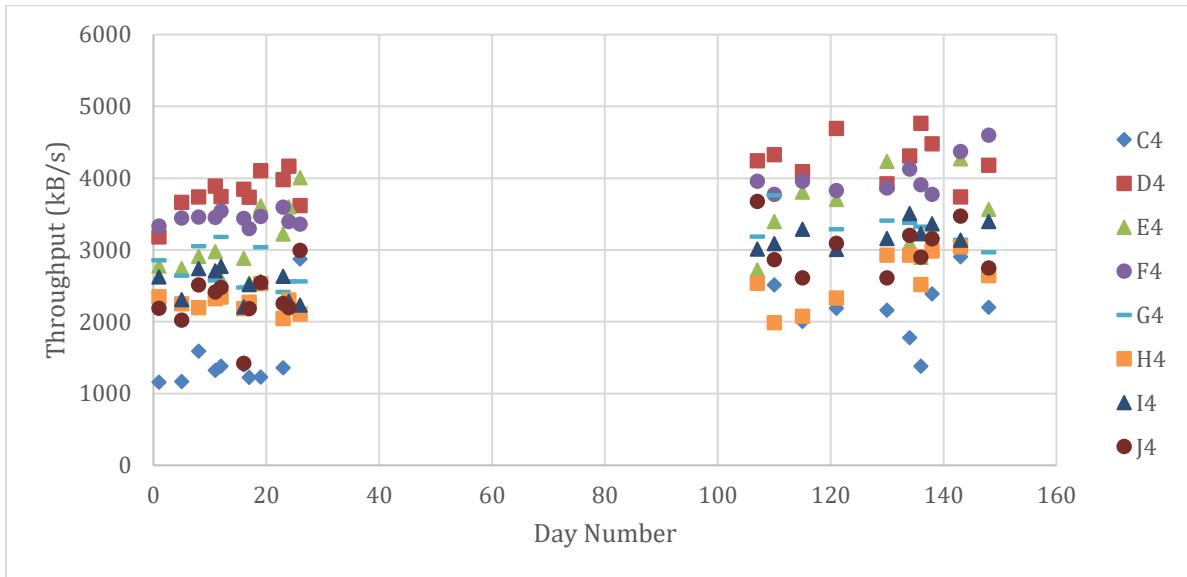
**Figure 5.7: Partial Low-Gain Antenna Throughput vs. Date
for Selected Sectors Along a Line of Constant Angle**
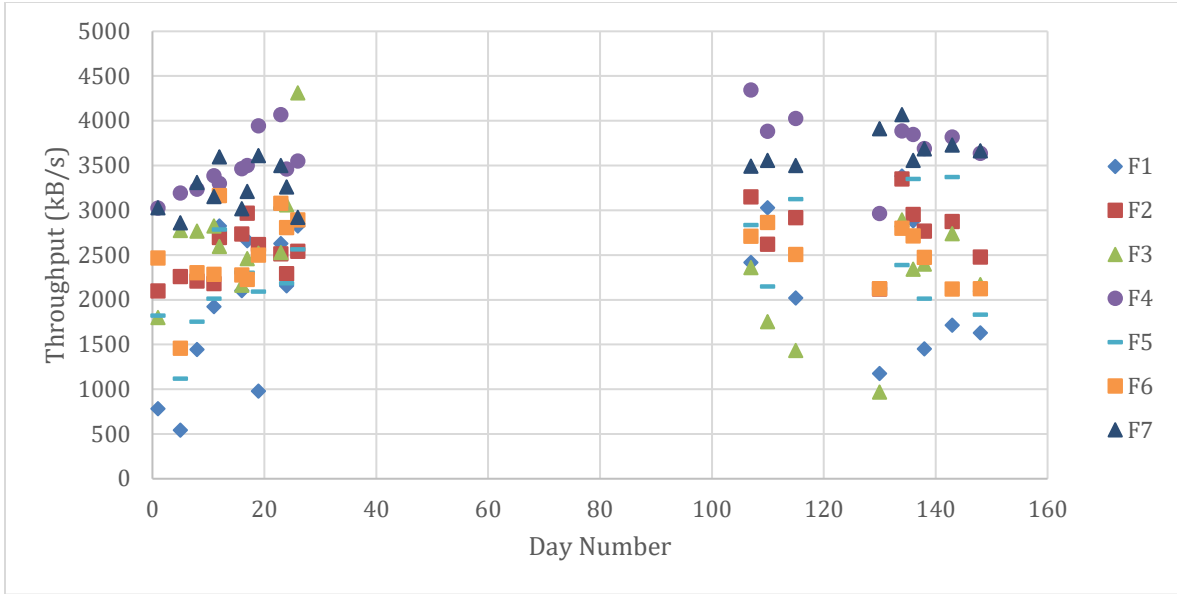
**Figure 5.8: Partial High-Gain Antenna Throughput vs. Date
for Selected Sectors Along an Arc of Constant Radius**
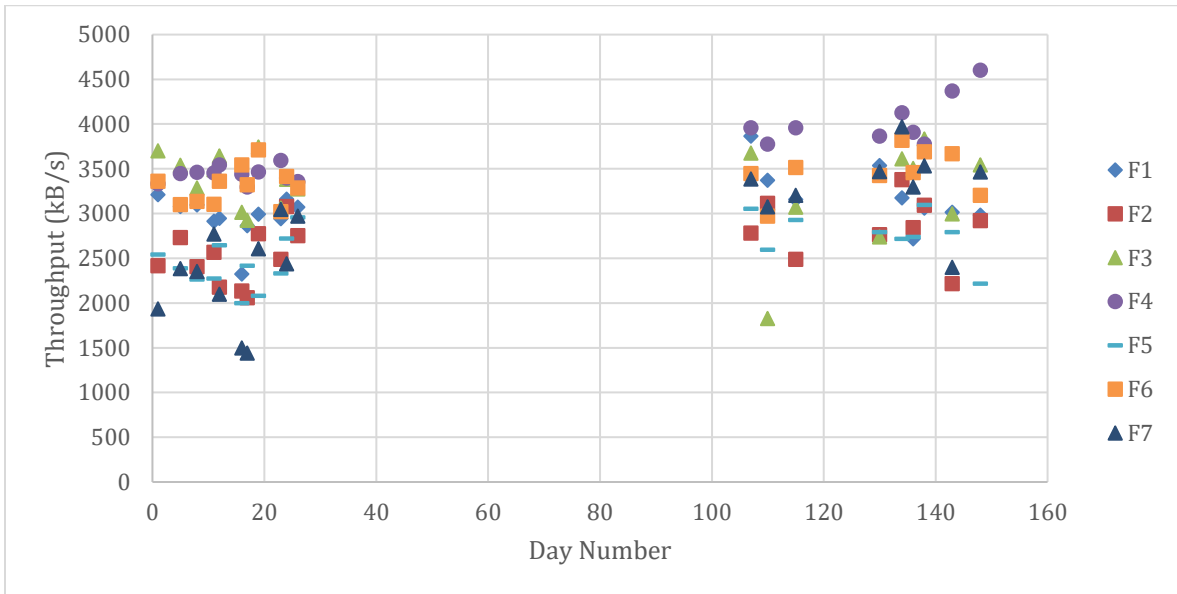
**Figure 5.9: Partial Low-Gain Antenna Throughput vs. Date
for Selected Sectors Along an Arc of Constant Radius**

It appeared in Figures 5.6 through 5.9 that while throughput may have slightly increased over the course of the growing season, the change was not significant. Figure 5.8 shows that as the tractor passed the center of the antenna's beamwidth (Radial 4) the throughput capacity was at its highest. To observe the purely time-influenced change in the overall throughput capacity of the system, the average of all sector averages was plotted as in Figure 5.10. The same data

74

plotting routine was used for the low gain antenna, as well as for the measurement of latency in the system. All of the raw data was imported in this manner before further analysis was conducted. The next step was to determine if any of the environmental characteristics, such as crop height, temperature, precipitation, position, and soil moisture had meaningful impacts on throughput or latency of any system.
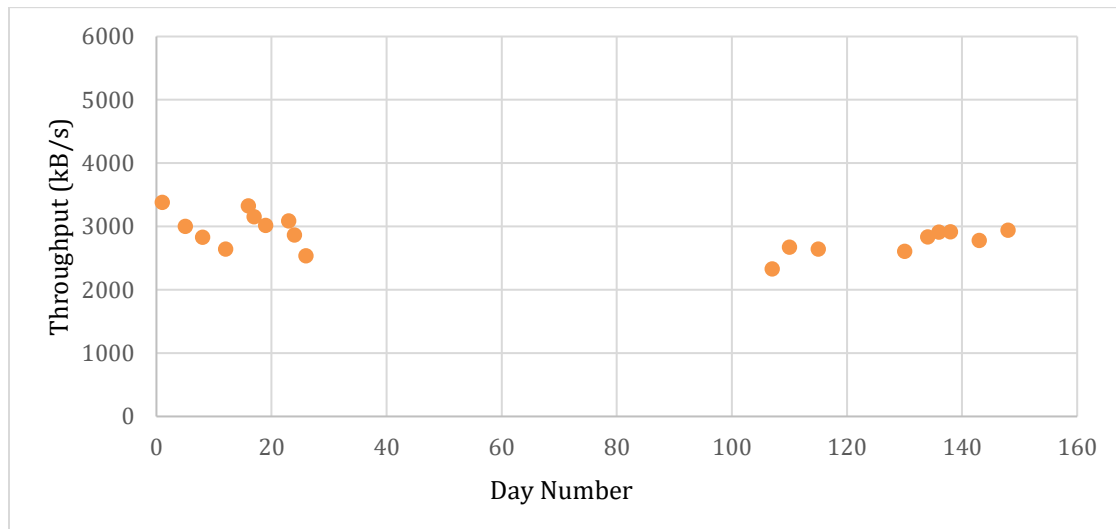
Figure 5.10: Mean Throughput of all Sectors vs. Date

It is important to note the units used in the charts above. The program iperf output data in units of kilobytes per second, whereas the typical convention for measurement of network throughput is megabit per second. The conversion is straightforward, as shown in Equation 5.4, but must be kept in mind when considering data shown in charts generated with iperf.

Eq. 5.4: $$T = TPT * 0.008$$

Where:

T = throughput in Mb/s

TPT = throughput in kB/s

5.4 Linear Regression Analysis

To explore relationships between the independent variables and network characteristics to both mobile (tractor) and stationary sensors, linear regression was used. The p-values of each coefficient indicated statistical significance for each corresponding predictor. Linear regression functions were generated for throughput, latency, and dropped packets.

5.4.1 Stationary Data

All collected sensor data was concatenated for each sensor. There were 9,634 readings. This meant appending each day's readings to the end of the previous day's readings to obtain a continuous list of readings from that particular sensor over the time while it was taking measurements. Weather data was retroactively added to this data, and a regression analysis performed. For the three network properties, each independent variable, a potential predictor, was evaluated independently to ascertain significance of effects. All data from the three sensors was concatenated to create one large list of sensor data. Whereas each sensor had been previously denoted by its identification number (1 through 3, from the access point to the fringe), now each sensor was denoted by its distance from the access point. These distances are seen in Table 5.1 below. The predictors at the time of analysis are given in Table 5.2. Dependent variables for regressions performed on both stationary and mobile sensor data are shown with their units in Table 5.3.

Table 5.1: Radial Distances of Each Sensor to the Access Point

Sensor	Distance
1	457 m (1500 ft)
2	853 m (2800 ft)
3	1189 m (3900 ft)

Table 5.2: Independent Variables (Predictors)
Used in Linear Regression Analysis of Stationary Sensor Data

Independent Variable	Measure
[DIST] Distance	[457, 853, 1189] meters
[DAY] Day	Integer Numeric from June 3rd
[PRCP] Precipitation	Decimal, centimeters
[YESTR] Previous Day's Precipitation	Decimal, centimeters
[2DPRCP] Previous Two Days' Precipitation	Decimal, centimeters
[3DPRCP] 3-Day Total Precipitation	Decimal, centimeters
[AVTEMP] Mean Temperature	Decimal, Celsius

Table 5.3: Dependent Variables Used in Linear Regression
Analysis of Both Stationary and Mobile Sensor Data

Dependent Variable	Measure
[TPT] Throughput	Kilobytes per Second [kB/s]
[LAT] Latency	Milliseconds [ms]
[DROP] Dropped Packets	Percentage [%]

Results of the analysis performed are shown in Equations 5.6 through 5.8, where each significant predictor of throughput, latency, and dropped packet data is shown. As described above, these predictors were each individually tested for significance with each significant previous predictor being included in a multivariate regression analysis. Correlation coefficients

of each model are also included as a measure of how well each network property was fit by the model. For all the tables presented below, the predictors were presented as part of a linear model that attempts to describe the network characteristic in question. These models take the form shown in Equation 5.5:

Eq. 5.5
$$Y = \beta_0 + \beta_1 X_1 + \beta_2 X_2 + \beta_3 X_3 + \cdots + \beta_n X_n$$

Where:

Y = Network Property (Throughput, Latency, Dropped Packets)

X_n = Predictor Input n (Distance, Day, etc.)

β_0 = Intercept Determined by Linear Regression

β_n = Coefficient Determined by Linear Regression

It should be noted that the predictors for each sensor that were significant (P-Value < 0.05) were not necessarily the same for all sensors. This led to a concern that the ability of these predictors to accurately describe network characteristics was not large. These predictors were watched in the final analysis of sensor data. The final round of analysis for sensor data was a total concatenation of sensor data, with a repetition of the analyses performed on individual sensors. Following progressive analysis of each predictor against each network characteristic as outlined above, models were created for each network characteristic of significant predictors. These can be seen in equations 5.6, 5.7, and 5.8. The significance of each of the predictors can be seen under each coefficient.

Eq. 5.6
$$TPT = 12100 - 48 * DAY - 120 * AVTMP - 0.64 * DIST \; ; R^2 = 0.34$$
$$(P < 0.001) \quad (P < 0.001) \quad (P < 0.001) \quad (P < 0.001)$$

Eq. 5.7
$$LAT = 2.57 - 0.002 * DIST + 0.032 * DAY - 0.26 * 3DPRCP \; ; R^2 = 0.082$$
$$(P = 0.07) \quad (P < 0.001) \quad (P = 0.001) \quad (P < 0.001)$$

Eq. 5.8
$$DROP = -0.025 + 2.16 * 10^{-5} * DIST \; ; R^2 = 0.012$$
$$(P < 0.001) \quad (P < 0.001)$$

Although the predictive power of the models are poor ($R^2 = 0.34$ in the best case), the coefficients DAY, AVTMP, and DIST were highly significant in the model for TPT (Eq. 5.4.1.2). Coefficient values did not seem unreasonable, as within their respective ranges they resulted in the model providing reasonable outputs of TPT. For example, the coefficient of DAY was -48. The first day of sensor data was recorded on day 135, and the last day of sensor data was recorded on day 162. Thus, the predictor would contribute negatively to the overall throughput of the system between -6,480 and -7,780 kB/s. DAY alone offsets the intercept of 12,100 kB/s by at minimum -6,480, resulting in a maximum possible throughput of 5,620 kB/s (45 Mb/s), which was roughly in the range of the readings taken. After DAY, the coefficient of AVTMP was -120. The range of AVTMP was between -2.6 and 17.4 degrees Celsius. Thus, the range of contribution to TPT was between -2,090 and 312 kB/s. Finally, DIST had a coefficient of -0.64, with a range of 457 to 1190 meters. The possible contribution to TPT from DIST was -760 to -293 kB/s. Therefore cumulatively, the range of possible TPT values ranged from 1,480 kB/s to 5,640 kB/s (11.8 Mb/s to 45.1 Mb/s), which was in the range of measurements taken.

According to the model (Eq. 5.4.1.3), latency was affected significantly by DIST, DAY, and 3DPRCP. The predictive power of the model was very poor at $R^2 = 0.082$. In a similar way to the explanation of Eq. 5.4.1.2 previously, the predictor coefficients' contributions to LAT were calculated. The intercept was 2.57ms, with DIST and its coefficient having a range of -2.380 ms to -0.914 ms. DAY and its coefficient had an impact of 4.32 ms to 5.18 ms. 3DPRCP and its coefficient had an impact on LAT between -0.936 ms and 0 ms. Thus, the total range of LAT was between 3.58 ms and 6.84 ms. The range for LAT was similar to the range of latencies measured.

The model describing the number of dropped packets (Eq. 5.4.1.4) followed suit with models generated from individual sensor data. It described the measured data extremely poorly, with a correlation coefficient of $R^2 = 0.012$, and had only one significant predictor: DIST. The coefficient on DIST was $2.16 * 10^{-5}$, with a model intercept of -0.025. Since DROP was measured in percentage of packets dropped, DROP represents the likelihood in percent of a packet being dropped. DIST contributed a range of 0.00988 to 0.0257 percent change increase of a dropped packet. Because of this, the model could provide a range of -1.5% to 0.068% chance of a particular packet being dropped. The regression's inclusion of negative percentages is not

consistent with real-world measurements and should therefore be set to 0% for all negative values. All results described here will be discussed further in Section 6.

5.4.2 Tractor Data

5,721 data points from the tractor were processed in the same way as data from the sensors. Since data was collected from the tractor both before and after the crops had stopped growing, crop height data was included in the list of potential predictors. Finer location data was also available for readings made from the tractor, as each data entry was tagged with a GPS location. These GPS coordinates were converted into polar coordinates, indicating the readings' location in angle from the access point and distance from the access point.

An assumption was made that the beam radiated by the access point was symmetrical, and aimed directly westward. As a result, the angular position information for each tractor reading was made positive. Since each angular measurement was positive, the effect of deviation from the center of the beam width could be measured on network properties. A table of information used as potential predictors for tractor data is shown in Table 5.4.

Table 5.4: Independent Variables (Predictors)
Used in Linear Regression Analysis of Mobile Data

Independent Variable	Measure
[ANT] Antenna	[0, 1] for High or Low Gain
[DIST] Distance	Decimal, meters
[ANGLE] Angle from Beam Center	Decimal, degrees
[DAY] Day	Integer Numeric from June 3rd
[CORN1] Corn 1 Height	Decimal, centimeters
[CORN2] Corn 2 Height	Decimal, centimeters
[SOY] Soybean Height	Decimal, centimeters
[PRCP] Precipitation	Decimal, centimeters
[YESTR] Previous Day's Precipitation	Decimal, centimeters
[2DPRCP] Previous Two Days' Precipitation	Decimal, centimeters

[3DPRCP] 3-Day Total Precipitation	Decimal, centimeters
[AVTEMP] Mean Temperature	Decimal, Celsius

       Results from the Excel regression analysis indicated that several factors contributed to throughput, latency, and dropped packets. Unfortunately, these factors failed to explain all but a small percentage of the total data population. Each predictor was individually regressed with each network characteristic to assess its individual relationship. Following this, all predictors were used to predict each characteristic, and those that were shown to be significant (P-Value < 0.05) were used to create a final model for each network parameter. The results of this regression test are shown as Equations 5.9, 5.10, and 5.11, where the significance of each coefficient is shown beneath.

Eq. 5.9 $TPT = 3480 - 0.45 * DIST - 18.6 * ANG + 1.65 * CORN1 \; ; R^2 = 0.09$
$\qquad\quad$ (P < 0.001)$\quad$(P < 0.001)$\quad$(P < 0.001)$\quad$(P < 0.001)

Eq. 5.10 $LAT = 3.5 + 1.24 * ANT + 0.039 * ANG + 0.006 * CORN2 \; ; R^2 = 0.006$
$\qquad\quad$ (P < 0.001)$\quad$(P = 0.001)$\quad$(P = 0.004)$\quad$(P < 0.001)

Eq. 5.11 $DROP = \; 0.016 - 0.003 * ANT - 0.0003 * DAY$
$\qquad\quad$ (P < 0.001)$\quad$(P < 0.001)$\quad$(P < 0.001)

$$+0.00018 * CORN1 - 0.00074 * AVTMP \; ; R^2 = 0.013$$
$\qquad\qquad\qquad\quad$ (P < 0.001)$\quad$(P < 0.001)

       Coefficients shown in Equation 5.9 describe the collected data poorly, with a correlation coefficient of only $R^2 = 0.09$. Each coefficient is highly significant, however. DIST, ANG, and CORN1 each had a p-value of less than 0.001, as well as the intercept of 3,480 kB/s. DIST had a range of 13m to 1,470m and therefore with its coefficient of -0.45 had an effect on TPT between -660 kB/s and -5.85 kB/s. ANG had a coefficient of -18.6 and a range of 0.228 degrees to 62.7 degrees, yielding an effect of -1,170 kB/s to -4.24 kB/s on TPT. Finally, CORN1 with its coefficient of 1.65 had a range of 7.62 cm to 259 cm, providing an effect of 12.6 kB/s to 427 kB/s of change on TPT. These coefficients allowed TPT to vary between 1,660 kB/s and 3,900 kB/s (13.3 Mb/s to 31.2 Mb/s). This range was appropriate for the readings taken.

Equation 5.10 described the latency (LAT) present during the experiment. Its ability to describe the data as a whole was very poor at $R^2 = 0.006$. However, each predictor had a significant coefficient. The predictors were ANT, ANG, and CORN2, with an intercept of 3.5ms. ANT was a binary variable, with a coefficient of 1.24. Therefore when the high gain antenna was in use (ANT = 1) there was a 1.24ms gain in latency. ANG had a coefficient of 0.039, and therefore contributed between 0.0089 ms and 0.24 ms of latency to LAT. Finally, CORN2 had a range of 8.89 cm to 260 cm with a coefficient of 0.006. It therefore contributed between 0.053 ms and 10 ms of latency to LAT. These predictors allowed the range of LAT to vary between 3.6 ms and 14.98 ms of latency. Given the large area the tractor covered, and the various surroundings it encountered throughout the planned route, this range seems acceptable and is in the same range as the collected data.

Finally, Equation 5.11 modeled the number of packets that were dropped by the tractor's communication system. ANT, DAY, AVTMP, and CORN1 were the predictors with acceptable significance ($P < 0.05$). As in Equation 5.8, DROP is measured in percentage change a packet will be dropped, with an intercept of 1.6%. ANT is a binary variable with coefficient -0.003, giving it a possible contribution of -0.3% when the high-gain antenna was used. DAY ranged from 1 to 148 and had a coefficient of -0.0003, giving it a contribution of between -4.4% and -0.03% chance of packet loss. CORN1 had a coefficient of 0.00018, giving it a range of 0.14% to 4.7%. AVTMP varied between 8.7 ⁰C and 28 ⁰C with a coefficient of -0.00074, giving it an effective range of 0.64% to 2.1% chance of packet loss. These predictors gave DROP a range of -2.3% to 8.4% chance of packet loss. Like Equation 5.8, the regression yields negative percentages; percentages cannot be below zero, so a model with an intercept of zero would have been more appropriate.

These results show that some factors affect throughput, latency, and dropped packets, but the generated models do a poor job of describing the data, as shown by each model's correlation coefficient. In the next section, the analysis presented here will be discussed. Full results of the regression on the project's data, including nonsignificant predictors, can be seen in the regression output tables located in Appendix D. Raw data from all sensors is available in Excel format on GitHub at https://github.com/thiemep/TPAC-Wifi .

5.5 Suitability of Linear Regression

As discussed in section 4.1, the data sent over a link using the 802.11 protocol is highly processed using a variety of encoding methods. Unlike channel sounding measurements like those discussed in section 2, the hardware used to transmit Wi-Fi data continuously measures signal strength and signal-to-noise ratio. Based on these measurements, it can choose different transmission schemes to ensure packet reception. Because of this, linear modeling was chosen as it was thought that any change in network characteristics would be small when a connection was present. If there was more variation in the dataset, exponential regression may have been used.

The models described in section 5.4 all had poor fit to the collected data. After analysis in this manner, the suitability of linear regressions to describe the data was called into question. Often in RF design and analysis work logarithmic scales are often used to display large ranges of values. This is the case when describing characteristics like RF loss, power, gain, and frequency. For this study linear regressions were used in place of exponential regressions due to the constraints of the system and the protocols used to send data.

As discussed earlier, there was little change in network characteristics throughout the season and throughout the area of interest. Latency remained well below acceptable levels, and throughput seldom dropped below 10 Mb/s. DIST, ANG, and DAY all seemed to have little effect on the actual measurements taken. Because of this, an exponential regression would likely have provided no better model than the linear regressions. Therefore, linear regressions were chosen to help identify independent variables that affected the dependent variables instead of creating a comprehensive model to be used for prediction. Greater distances, wider angles, and longer testing times are required to stretch the capabilities of the system to a fuller extent. Data gathered from these more strenuous tests may show a drop in throughput, a rise in latency, and an increased number of lost packets that could be used; with this data, perhaps exponential regression may yield a useful predictive model of network characteristics.

6. CONCLUSIONS

6.1 Completion of Research Goals

At the project's outset, the prospect of creating a usable 2.4Ghz Wi-Fi system for use in wide-area outdoor environments was to be studied. To parameterize the effectiveness of this system, three requirements needed to be met for the system to qualify as usable:

1. throughput had to consistently remain above 1Mb/s;
2. the connection had to present latency to the network of under 500 milliseconds;
3. equipment used had to be able to endure prolonged outdoor / agricultural use; and
4. determine effect, if any, of environmental changes on connection properties.

Based upon the throughput measured over the course of the growing season, a sample of which was shown in Figures 5.6 through 5.9, and based upon the latency presented to the client that never exceeded 100ms, requirements 1 and 2 were satisfied. Multiple linear regression analysis of the data was pursued to ascertain environmental effects on connectivity – but these results were inconclusive. Crop growth, ambient temperature, precipitation, and antenna gain all had statistically significant effects on network characteristics, but the models had poor correlation and the network characteristics in all spaces throughout the growing season were largely uniform. Since the entire area of interest was exposed to the access point via line-of-sight, that this experiment showed that line-of-sight was a more important predictor of network connection ability than any of the independent variables.

Despite the loss of the tower access point mid-way through the season, this work showed that off-the-shelf network equipment be robust enough to withstand agricultural use. The access point radio had damage to its LAN speed controller which caused it to improperly negotiate ethernet connection speeds with the router, locking the wired speed to 10Mb/s. Under normal circumstances, the Ubiquiti Bullet is capable of communicating with the router up to 100 Mb/s. This damage caused enough of a bottleneck in the system to rate limit iperf's ability to test the network speed. Thus all the data having the steady 10 Mb/s throughput reading was omitted. Every other component in the system, from the mobile sensor to every component in the field

sensors, performed flawlessly in conditions from mid-summer to below freezing, and from very dry conditions to the wet conditions experienced through late spring. This high reliability record, coupled with the unconventional placement of the access point on a 120m (400ft) broadcast tower prone to lightning strikes, warranted the incident's exception and the completion of the third network requirement that the equipment stand up to agricultural use.

Inspection of the models generated by multiple linear regression, showed that none fit their dependent variables well. The largest correlation coefficient shown in the project was $R^2 = 0.34$, which was found on the throughput regression for stationary sensors. This widespread lack of correlation does not mean that the models are unusable. Many of the statically significant coefficients mirror what results would be expected from an increase or decrease in a particular parameter. In future work with an expanded system, linear regressions could be accompanied by exponential regressions.

The models generated by the analysis of collected data were not powerful, and unable to demonstrate and meaningful relationship between independent and dependent variables. Since no independent variables stood out as obvious contributors to change in either throughput, latency, or the number of dropped packets, the goals set forth for the project were met, specifically:

1. It was determined that antenna gain had no significant effect on any network property
2. No meaningful relationships were found between weather conditions or crop heights and network properties
3. No relationships were uncovered between time of the year and network properties

Because no meaningful relationships were found between antenna gain, environmental conditions, crop height, or time of year to network properties, these conditions would have little or no effect on throughput, latency, or the number of dropped packets in this setting. Conventional wisdom for setting up outdoor systems in the 2.4GHz band and above has been that if line of sight is available between the base station and the client, that a connection will be possible and relatively stable. The results of this paper support that convention.

6.2 Future Work

Further research in this area should be performed at locations with greater acreage. While there were some changes in throughput with distance, they were not appreciable. Because of this lack of fluctuation in speeds, this system could be taken much further from the access point to cover a larger area. This project was limited by the spaces available, and would likely have shown more interesting results had the client and sensors been able to connect at a greater distance, as would be the case with a larger production farm.

This work showed that a 2.4GHz wireless network is not only feasible on a production farm, but that is has the capability to cover very large areas with high speed wireless connectivity. The importance of finding the limits of such a system are imperative to the understanding of the capabilities of such a system. Finding the "fringes" of the coverage area, observing what happens to network properties at extreme distances, and observing these properties in fringe areas under adverse weather conditions would likely shed light on the limits of current commercial 2.4GHz technology for agricultural use.

Additionally, the inclusion of terrain with more obstacles would allow observations to be made of network behavior due to blockages in line-of-sight. As mentioned previously, the conventional wisdom when designing networks of this frequency and higher is that line-of-sight is key to a stable connection. In agricultural applications, particularly in parts of the world where altitude changes exist, these blockages to line-of-sight are unavoidable. Such terrain would also highlight the potential effect of antenna gain on signal properties, as changes in vehicle pitch would cause radiation to over-shoot or under-shoot the access point in line-of-sight conditions. For this, a mirror experiment should be conducted in an area with mountainous, forested, or hilly terrain.

BIBLIOGRAPHY

Antonis Tzounis, N. K. (2017). Internet of Things in Agriculture, Recent Advances and Future Challenges. *Biosystems Engineering 164*.

Bevelacqua, P. J. (2011). *The Monopole Antenna*. From Antenna Theory: http://www.antenna-theory.com/antennas/monopole.php

Chew, W. C. (1990). *Waves and Fields in Inhomogenous Media.* IEEE Press.

Dekleva, S. (2007). Evolving and Emerging Issues in Mobile Wireless Networks. *Communications of the ACM - Smart Business Networks* (pp. 38-43). ACM New York.

H. Wu, Y. M. (2015). Empirical Modeling and Evaluation of Multi-Path Radio Channels on Wheat Farmland Based on Communication Quality. *Information, Technology, Sensors, and Control Systems Community of ASABE*.

Hintersteiner, J. D. (2017). *Antennas: Why They Matter and When You Want to Use APs with Internal vs. External Antennas*. From Emperor Wi-Fi: http://www.emperorwifi.com/2017/11/antennas-why-they-matter-and-when-do.html

Ingenu Inc. (2018). From RPMA Technology: https://www.ingenu.com/technology/rpma/

Jangeun Jun, P. P. (2003). Theoretical Maximum Throughput of IEEE 802.11 and its Applications. *Proceedings of the Second IEEE International Symposium on Network Computing and Applications.* IEEE.

Jean-Christophe, Z. (2013). Aerial Collective Systems. *Handbook of Collective Robotics*, 18.

John Deere and Company. (2018). *JDLink*. From https://www.deere.com/en/technology-products/precision-ag-technology/data-management/jdlink/

Keysight Technologies. (2018). *FieldFox Handheld RF and Microwave Analyzers.* From https://www.keysight.com/en/pcx-x205201/fieldfox-handheld-rf-and-microwave-analyzers?&cc=US&lc=eng

LoRa Alliance. (2018). From LoRa Alliance: https://lora-alliance.org/

M. J. Darr, L. Z. (2008). A Model for Predicting Signal Transmission Performance of Wireless Sensors in Poultry Layer Facilities. *Information and Electrical Trchnologies Division of ASABE*.

McMahon, R. (2018). *iPerf - The Ultimate Speed Test Tool for TCP, UDP, and SCTP*. From Iperf: https://iperf.fr/iperf-download.php

Motorola Solutions. (2005). *Standards and Guidelines for Communication Sites.* From United States Bureau of Land Management: https://www.blm.gov/sites/blm.gov/files/Lands_ROW_Motorola_R56_2005_manual.pdf

Myers Engineering. (2008). *Type N Cable Assemblies.* From
https://www.myerseng.com/coaxial-cables/Coaxial-Cables-Atten-imperial-26k.gif

Primus Cable. (2018). *CAT6 Bulk Stranded Ethernet Cable, Shielded Bare Copper*. From Primus
Cable: https://www.primuscable.com/store/p/9452-CAT-6-Ethernet-Cable-Indoor-
Shielded-Stranded-Copper-24-AWG.aspx

Purdue University Open Agricultural Technology and Systems Center. (2018). *ISOBlue 2.0.*
From ISOBlue: www.isoblue.org

R. A. Rohrer, J. D. (2018). Evaluation of the Accuracy of Machine Reported CAN Data for
Engine Torque and Speed. *Machinery Systems Community of ASABE.*

R. S. Freeland, M. J. (2014). PRecision Agriculture: RTK Base-to-Tractor Range Limitations
Using RF Communication. *Information and Electrical Technologies Division of ASABE.*

Raspberry Pi Foundation. (2012). *Raspberry Pi 3 Model B+*. From
https://static.raspberrypi.org/files/product-briefs/Raspberry-Pi-Model-Bplus-Product-
Brief.pdf

Seco SPA. (2018). *Uxoo X86 II*. From Udoo: https://www.udoo.org/udoo-x86/

Sharony, J. (2006). *Introduction to Wireless MIMO - Theory and Applications.* IEEE.

Sigfox. (2018). From Sigfox: https://www.sigfox.com/en

Solinftec. (2018). From Solinftec: http://solinftec.com/

TerraWave Solutions Inc. (n.d.). *TerraWave Solutions 2.4GHz 18dBi 65 Degree Cross-Polarized
Panel Antenna with N-Style Jack Connectors.* From Ventev:
https://www.ventevinfra.com/shop/files/products/antennasb/24-ghz-antennas/24-ghz-
sector-panel-
antennas/2.4%20GHz%2018%20dBi%2065%20Degree%20Cross%20Pol%20Panel%20
Antenna_T24180P10006-65X.pdf

Ubiquiti Networks Inc. (2011). Bullet M.

U-Blox, Inc. (2018). *u-blox 7 Receiver Description.* From https://www.u-
blox.com/sites/default/files/products/documents/u-blox7-
V14_ReceiverDescriptionProtocolSpec_%28GPS.G7-SW-12001%29_Public.pdf

United States Federal Communications Commission. (2019). Title 47 Part 15.

United States National Oceanic and Atmospheric Administration. (2019). *Climate Data Online*.
From NOAA National Centers for Environmental Information:
https://www.ncdc.noaa.gov/cdo-web/

Z. Li, N. W. (2010). Radio Path-Loss Modeling for a 2.4GHz In-Field Wireless Sensor Network.
Information and Electrical Technologies Division, ASABE.

Zhang, Q. (2015). *Precision Agriculture Technology for Crop Farming.* CRC Press.

Zigbee Alliance. (2018). From Zigbee Alliance: zigbeealliance.org

APPENDIX A. BILL OF MATERIALS

The table contained in this appendix documents all hardware used in this work. Existing structures, vehicles, consumables like fuel, and services like hiring tower climbers are not included in this section. The table is divided into three sections, one for each system.

Item	Quantity	Unit Price (USD)	Total Price (USD)
FIELD SENSORS	------------------------	-------------------------	-------------------------
Udoo x86	3	206.7	620.10
NEMA Enclosure	3	49.99	149.97
PoE Injector	3	52.05	156.15
Ubiquiti Bullet M2	3	72.90	218.70
Fence Post	3	2.49	7.47
8dB Antenna	3	43.99	131.97
12V Battery	6	69.99	419.94
Battery Cables	3	7.90	23.70
3' Ethernet Cables	6	1.80	10.80
		SUBTOTAL:	1,738.80
MOBILE SENSOR	------------------------	-------------------------	-------------------------
Udoo x86	1	206.7	206.70
PoE Injector	1	Included	0.00
Ubiquiti Bullet M2	1	72.90	72.90
8dB Antenna	1	43.99	43.99
15dB Antenna	1	124.98	124.98
Power Inverter	1	29.99	29.99
RF Switch	1	200	200.00
LMR 400 Cable	1 (Spool, 100ft)	100	100.00
Male N-Connector	2	3.58	7.16
Female N-Connector	2	5.50	11.00
3' Ethernet Cable	2	1.80	3.60
GPS Module	1	15.99	15.99
N-to-SMA Adapter	3	8.99	26.97

		SUBTOTAL:	843.19
ACCESS POINT	------------------------	------------------------	------------------------
Dell R230 Server	1	819.29	819.29
Ubiquiti ER-X-SFP	1	73.80	73.80
Shielded Ethernet	1 (Spool, 500ft)	133.76	133.76
Male Ethernet Jacks	1 (Pack, 50)	7.99	7.99
Ethernet Cable Boots	1 (Pack, 100)	6.96	6.96
Ubiquiti Bullet M2	1	72.90	72.90
Ubiquiti PBE-5AC-GEN2	2	135	270.00
Terrawave Antenna	1	190.54	190.54
Tower Climber Service (Visit)	4	300	1200.00
Ethernet Surge Protector	3	16.69	50.07
		SUBTOTAL:	2,555.31
		TOTAL:	**5,137.30**

APPENDIX B. NETWORK SETTINGS

The tables given in this section provide all relevant settings used in the Ubiquiti networking equipment. These settings were set using the web-based configuration tool that is enabled by default on all modern Ubiquiti network components. Tables are divided by component, with each providing the setting, the amount the setting was set to, and the units of each setting, when applicable.

Access Point Transceiver Settings for Ubiquiti Bullet M2

Setting:	Amount:	Measure:
Output Power	18	dBm
Channel Width	20	MHz
Channel / Frequency	2 / 2417	Channel / MHz
Maximum TX Rate	65 / 72.2	Mb/s
Security	WPA2-AES	N/A
Network Mode	Bridge	N/A
Multicast Data	Allow	N/A
Multicast Enhancement	Enable	N/A
LAN Speed	100 / Auto	Mb/s

Client Transceiver Settings for Ubiquiti Bullet M2

Setting:	Amount:	Measure:
Output Power	28 (Stationary) / 21 (Tractor)	dBm
Channel Width	20	MHz
Channel / Frequency	2 / 2417	Channel / MHz
Maximum TX Rate	65 / 72.2	Mb/s
Security	WPA2-AES	N/A
Network Mode	Station	N/A
Multicast Data	Allow	N/A

Multicast Enhancement	Enable	N/A
LAN Speed	100 / Auto	Mb/s

APPENDIX C. LIST OF TERMS

The area of wireless communications uses many acronyms. For those readers who may not work in the field, or who are unfamiliar with certain acronyms used in this work, this table was created. It is meant to contain the spelled-out meanings of all acronyms used in this paper.

AoI	Area of Interest	LMR400	Coaxial Cable
CAN	Controller Area Network	MATLAB	Matrix Laboratory (Software)
CANBUS	Controller Area Network Bus	MIMO	Multiple-In Multiple-Out
CCK	Complimentary Code Keying	NEMA	National Electrical Manufacturers Association
CSV	Comma Separated Value		
dB	Decibels	NOx	Oxides of Nitrogen
dBi	Decibels (isotropic)	OFDM	Orthogonal Frequency-Division Multiplexing
dBm	Decibel-Milliwatts		
DEF	Diesel Exhaust Fluid	PoE	Power over Ethernet
DOT	Department of Transportation	RF	Radio Frequency
DPSK	Differential Phase Shift Keying	SMA	SubMiniature Version A (Connector)
ECU	Engine Control Unit	SPDT	Single Pole Double Throw
ERP	Estimated Radiated Power	SSH	Secure Shell
FCC	Federal Communications Commission	SWR	Standing Wave Ratio
FM	Frequency Modulation	TCP	Transmission Control Protocol
GMO	Genetically Modified Organism	TPAC	Throckmorton Purdue Agricultural Center
GPS	Global Positioning System	UDP	User Datagram Protocol
I/O	Inputs and Outputs (Pins on a Computer)	USB	Universal Serial Bus
IoT	Internet of Things	UV	Ultraviolet
IP	Internet Protocol	WAAS	Wide Area Augmentation System
ISM	Industrial, Scientific, and Medical	WBAA	Purdue's NPR Station
LIDAR	Light Detection and Ranging	WISP	Wireless Internet Service Provider

APPENDIX D. TABULAR RESULTS OF LINEAR REGRESSIONS

The tables provided in this section are the raw outputs of the multiple linear regression performed on the data collected from the stationary and mobile sensors. It is provided for reference purposes and includes more statistical information than was discussed in the results section.

Part 1: Stationary Sensor Regression Outputs

Regression Statistics

Multiple R	5.850E-01
R Square	3.423E-01
Adjusted R Square	3.419E-01
Standard Error	7.732E+02
Observations	5.720E+03

ANOVA

	df	SS	MS	F	Significance F
Regression	3.000E+00	1.778E+09	5.927E+07	9.915E+02	0.000E+00
Residual	5.716E+03	3.417E+09	5.978E+05		
Total	5.719E+03	5.195E+09			

	Coefficients	Standard Error	t Stat	P-value	Lower 95%	Upper 95%	Lower 95.0%	Upper 95.0%
Intercept	1.213E+04	3.772E+02	3.215E+01	0.000E+00	1.139E+04	1.287E+04	1.139E+04	1.287E+04
Day	-4.819E+01	2.605E+00	-1.850E+01	3.046E-74	-5.329E+01	-4.308E+01	-5.329E+01	-4.308E+01
AvTMP (degC)	-1.193E+02	2.572E+00	-4.640E+01	0.000E+00	-1.244E+02	-1.143E+02	-1.244E+02	-1.143E+02
Sensor (m)	-6.416E-01	3.758E-02	-1.707E+01	8.545E-64	-7.153E-01	-5.679E-01	-7.153E-01	-5.679E-01

Figure D.1: Regression Table of Most Significant Independent Variables for Throughput in Stationary Sensors

Regression Statistics

Multiple R	2.862E-01
R Square	8.193E-02
Adjusted R Square	8.145E-02
Standard Error	2.315E+00
Observations	5.720E+03

ANOVA

	df	SS	MS	F	Significance F
Regression	3.000E+00	2.735E+03	9.117E+02	1.700E+02	1.352E-106
Residual	5.716E+03	3.065E+04	5.361E+00		
Total	5.719E+03	3.338E+04			

	Coefficients	Standard Error	t Stat	P-value	Lower 95%	Upper 95%	Lower 95.0%	Upper 95.0%
Intercept	2.568E+00	1.454E+00	1.767E+00	7.734E-02	-2.816E-01	5.418E+00	-2.816E-01	5.418E+00
Sensor (m)	-1.950E-03	1.143E-04	-1.706E+01	1.091E-64	-2.174E-03	-1.726E-03	-2.174E-03	-1.726E-03
Day	3.226E-02	1.020E-02	3.162E+00	1.576E-03	1.226E-02	5.227E-02	1.226E-02	5.227E-02
3DPRCP (cm)	-2.590E-01	3.159E-02	-8.199E+00	2.978E-16	-3.209E-01	-1.970E-01	-3.209E-01	-1.970E-01

Figure D.2: Regression Table of Most Significant Independent Variables for Latency in Stationary Sensors

Regression Statistics

Multiple R	1.112E-01
R Square	1.237E-02
Adjusted R Square	1.226E-02
Standard Error	5.635E-02
Observations	9.363E+03

ANOVA

	df	SS	MS	F	Significance F
Regression	1.000E+00	3.723E-01	3.723E-01	1.172E+02	3.667E-27
Residual	9.361E+03	2.973E+01	3.175E-03		
Total	9.362E+03	3.010E+01			

	Coefficients	Standard Error	t Stat	P-value	Lower 95%	Upper 95%	Lower 95.0%	Upper 95.0%
Intercept	-2.146E-02	-2.146E-02	-2.146E-02	-2.146E-02	-2.146E-02	-2.146E-02	-2.146E-02	-2.146E-02
Sensor (m)	2.549E-05	2.549E-05	2.549E-05	2.549E-05	2.549E-05	2.549E-05	2.549E-05	2.549E-05

Figure D.3: Regression Table of Most Significant Independent Variables for Dropped Packets in Stationary Sensors

Part 2: Mobile Client Regression Outputs

SUMMARY OUTPUT

Regression Statistics

Multiple R	2.997E-01
R Square	8.979E-02
Adjusted R Square	8.932E-02
Standard Error	1.091E+03
Observations	5.720E+03

ANOVA

	df	SS	MS	F	Significance F
Regression	3.000E+00	6.711E+08	2.237E+08	1.880E+02	3.025E-116
Residual	5.716E+03	6.803E+09	1.190E+06		
Total	5.719E+03	7.474E+09			

	Coefficients	Standard Error	t Stat	P-value	Lower 95%	Upper 95%	Lower 95.0%	Upper 95.0%
Intercept	3.478E+03	5.291E+01	6.572E+01	0.000E+00	3.374E+03	3.581E+03	3.374E+03	3.581E+03
Distance (m)	-4.535E-01	4.890E-02	-9.274E+00	2.477E-20	-5.493E-01	-3.576E-01	-5.493E-01	-3.576E-01
Angle (abs)	-1.854E+01	9.961E-01	-1.861E+01	4.478E-75	-2.049E+01	-1.658E+01	-2.049E+01	-1.658E+01
Corn1 (cm)	1.658E+00	1.293E-01	1.282E+01	4.096E-37	1.405E+00	1.912E+00	1.405E+00	1.912E+00

Figure D.4: Regression Table of Most Significant Independent Variables for Throughput in Mobile Client

SUMMARY OUTPUT

Regression Statistics	
Multiple R	7.454E-02
R Square	5.557E-03
Adjusted R Square	5.035E-03
Standard Error	1.466E+01
Observations	5.720E+03

ANOVA

	df	SS	MS	F	Significance F
Regression	3.000E+00	6.866E+03	2.289E+03	1.065E+01	5.617E-07
Residual	5.716E+03	1.229E+06	2.150E+02		
Total	5.719E+03	1.236E+06			

	Coefficients	Standard Error	t Stat	P-value	Lower 95%	Upper 95%	Lower 95.0%	Upper 95.0%
Intercept	3.476E+00	4.627E-01	7.514E+00	6.641E-14	2.569E+00	4.383E+00	2.569E+00	4.383E+00
Ant	1.242E+00	3.886E-01	3.196E+00	1.400E-03	4.802E-01	2.004E+00	4.802E-01	2.004E+00
Angle (abs)	3.878E-02	1.333E-02	2.909E+00	3.641E-03	1.265E-02	6.492E-02	1.265E-02	6.492E-02
Corn2 (cm)	6.038E-03	1.736E-03	3.478E+00	5.090E-04	2.634E-03	9.441E-03	2.634E-03	9.441E-03

Figure D.5: Regression Table of Most Significant Independent Variables for Latency in Mobile Client

SUMMARY OUTPUT

Regression Statistics	
Multiple R	1.126E-01
R Square	1.268E-02
Adjusted R Square	1.199E-02
Standard Error	3.104E-02
Observations	5.720E+03

ANOVA

	df	SS	MS	F	Significance F
Regression	4.000E+00	7.070E-02	1.768E-02	1.835E+01	5.412E-15
Residual	5.715E+03	5.505E+00	9.632E-04		
Total	5.719E+03	5.575E+00			

	Coefficients	Standard Error	t Stat	P-value	Lower 95%	Upper 95%	Lower 95.0%	Upper 95.0%
Intercept	1.519E-02	2.666E-03	5.696E+00	1.286E-08	9.960E-03	2.041E-02	9.960E-03	2.041E-02
Ant	-2.837E-03	8.273E-04	-3.430E+00	6.089E-04	-4.459E-03	-1.215E-03	-4.459E-03	-1.215E-03
Day	-2.943E-04	7.044E-05	-4.178E+00	2.989E-05	-4.324E-04	-1.562E-04	-4.324E-04	-1.562E-04
Corn1 (cm)	1.175E-04	3.421E-05	3.436E+00	5.948E-04	5.048E-05	1.846E-04	5.048E-05	1.846E-04
AVTMP (°C)	-7.357E-04	1.244E-04	-5.913E+00	3.548E-09	-9.796E-04	-4.918E-04	-9.796E-04	-4.918E-04

Figure D.6: Regression Table of Most Significant Independent Variables for Dropped Packets in Mobile Client